Georgia State University
ScholarWorks @ Georgia State University

Chemistry Theses | Department of Chemistry

11-3-2008

Electrochemical Studies of Substituted Anthraquinones

Daniel Joshua Rabinowitz

Follow this and additional works at: http://scholarworks.gsu.edu/chemistry_theses

Recommended Citation
Rabinowitz, Daniel Joshua, "Electrochemical Studies of Substituted Anthraquinones" (2008). *Chemistry Theses.* Paper 15.

This Thesis is brought to you for free and open access by the Department of Chemistry at ScholarWorks @ Georgia State University. It has been accepted for inclusion in Chemistry Theses by an authorized administrator of ScholarWorks @ Georgia State University. For more information, please contact scholarworks@gsu.edu.

ELECTROCHEMICAL STUDIES OF SUBSTITUTED ANTHRAQUINONES

By

Daniel Joshua Rabinowitz

Under the Direction of Thomas L. Netzel

ABSTRACT

Electrochemical potentials of a series of anthraquinone derivatives were studied in both aqueous solution and acetonitrile. The long term goal of this work was to find derivatives which could be reduced easily for studies of photoinduced electron transfer in DNA. Our immediate goal was to find the substitution group that gave the least negative redox potential value. Of all derivatives studied, the anthraquinone imides as a class had the least negative redox potentials, in the range of -0.600 to -0.550 V vs. SCE. One of the anthraquinones studied, one derivative (deoxyadenosine conjugated with an ethynyl linker to an anthraquinone with two ester substituents) was also in this range. A study of a series of anthraquinones conjugated with ethynyl and ethanyl linkers showed that the ethynyl linker was more effective than the ethanyl linker in lowering the redox potential of anthraquinone.

INDEX WORDS: Anthraquinone, electron-withdrawing group, acetonitrile, water, redox potentials, ethynyl linker, ethanyl linker, Saturated Calomel Electrode.

ELECTROCHEMICAL STUDIES OF SUBSTITUTED ANTHRAQUINONES

by

Daniel Joshua Rabinowitz

A Thesis Submitted in Partial Fulfillment of the Require for the Degree of

Master of Science

In the College of Arts and Sciences

Georgia State University

2008

Copyright by
Daniel Joshua Rabinowitz
2008

ELECTROCHEMICAL STUDIES OF SUBSTITUTED ANTHRAQUINONES

by

Daniel Joshua Rabinowitz

Committee Chair: Thomas L. Netzel
Committee Co-Chair: Dabney W. Dixon

Committee: Jerry Smith
Gangli Wang

Electronic Version Approved:

Office of Graduate Studies
College of Arts and Sciences
Georgia State University
December 2008

DEDICATION

To my wife, Heather Rabinowitz, thank you for all of your moral support during my times of upheaval with research. You have guided me through difficult times, and with that, I honor you in my work.

I dedicate this thesis to my mother, Amy Rabinowitz, if it were not for her; I would have never completed my masters Degree. Thank you for listening to me, and making me continue the degree when I wanted to quit.

Frankie and Hannah you have been two supporting cast members, and have made sure that I finish my research and the thesis.

This work is dedicated to Thomas L. Netzel who passed away from prostate cancer on September 4, 2008. He was always happy, energetic and ready to take on any obstacle. It was a pleasure above all others to have worked with him. You will be missed more than you'll ever know. You helped me through the first six months of research, and weren't too upset with me when I had focused primarily on my courses. Your family holds onto a special part of my heart that no one will ever be able to take over. Thank you so much for entering my life, and I will always think of the movie real genius, when it comes to your laser lab.

ACKNOWLEDGEMENTS

I would like to acknowledge Dr. Netzel for providing me with the opportunity to do research in his laboratory. For buying me new electrodes when I broke them and for helping me troubleshoot CV issues.

Dr. Dixon, you have helped me write the thesis. I appreciate all of your help, you've been a driving force to the conclusion of this project.

I would like to thank Yu Cao, Reham Abou-Elkhair for providing me with all the anthraquinone compounds.

Dr. Smith you have always given me a sense of accomplishment and the fuel to improve myself throughout your courses. It has been a pleasure to work for you in CHEM 4000, and I hope that you have more TA's that help you.

I would like to thank Robert for all of his help with researching anthraquinone redox potentials on scifinder and Beilstein. It was a difficult task to find previous studies on anthraquinones, but you did the impossible, and found a lot of journals with me.

TABLE OF CONTENTS

DEDICATION iv

ACKNOWLEDGEMENTS v

LIST OF FIGURES ix

LIST OF TABLES xi

LIST OF ABBREVIATIONS xii

CHAPTER

1 Introduction 1

1.1 References 4

2 The Experimental Protocol 7

2.0 Introduction 7

2.1 Materials and Methods 7

2.1.1 Preparation of Solutions 8

2.1.2 The Procedure for Making Ag/AgCl/Cl^- Reference Electrode 8

2.1.3 The Procedure for Polishing the Working Electrode 9

2.1.4 The Procedure for Cleaning the Auxiliary Electrode 9

2.1.5 Preparation of Anthraquinones in Aqueous Solutions 9

2.2 Cyclic Voltammograph 10

2.2.1 Applying Electrochemistry for Aqueous Solutions 10

2.2.2 Confirming the XY Recorder was Working Properly 10

2.2.3 Calculating Redox Potentials from CV 11

2.2.4 Ferrocene Hexafluorophosphate and Ag/AgCl/NaCl (3 M) Reference Electrode 11

2.3 Results and Discussion 11

2.3.1 Selection of Electrode 11

2.3.2 Reduction of Anthraquinone 12

2.4 References 13

3 Study of Substituted Anthraquinones in CH_3CN 28

3.0 Introduction 28

3.1 Materials and Methods 29

3.1.1 Procedure for Making 0.10 M TBAH CH_3CN Solution 29

3.1.2 Procedure for Making 0.010 M Silver Nitrate ($AgNO_3$) in 0.10 M TBAH CH_3CN Solution 30

3.1.3 Preparation and Assembly of ANE2 Electrode 30

3.1.4 Ferrocene Internal Standard for CH_3CN Solutions 31

3.1.5 Redox Potential Values for Ferrocene in 0.1 M TBAH CH_3CN 31

3.2 Preparation of the Anthraquinone Samples in 0.1 M TBAH CH_3CN 31

3.3 Cyclic Voltammetry of Substituted Anthraquinone Samples in 0.1 M TBAH CH_3CN 31

3.4 Results and Discussion 32

3.4.1 Redox Potentials of Anthraquinones in 0.1 M TBAH CH_3CN 32

3.4.2 Anthraquinone Carboxamide Derivatives 33

3.4.3 Deoxyadensoine Ethanyl Anthraquinone-2,3-dimethyl ester 33

3.4.4 Anthraquinone Carboxylic Acid Derivatives 33

3.4.5 Anthraquinone $COCF_3$ and its Hydrated Form 34

3.4.6 The Effects of an Ethynyl Group on AQ Redox Potentials 35

3.4.7 Comparing Anthraquinone Covalently Linked (Ethynyl or Ethanyl) with dA 35

3.4.8 Ethylyn Linked Anthraquinone with Deoxyadenosine and Deoxyuracil 36

3.5 References 36

4 Synthesis, Electrochemistry and Hydrolysis of Anthraquinone Derivatives 52

4.0 Abstract 52

4.1 Keywords 52

4.2 Introduction 52

4.3 Results and Discussion 53

4.4 Experimental 54

4.4.1 Materials and General Methods 54

4.4.2 Electrochemistry 55

4.4.3 Synthesis 55

4.5 Acknowledgments 57

4.6 References 57

5 Theory and Experiment 66

5.0 Introduction 66

5.1 Methods 66

5.1.1 Gaussian 03 66

5.1.2 Calculation of Electron Affinity 66

5.2 Results and Discussion 67

5.3 References 68

6 Conclusions 74

LIST OF FIGURES

Figure 2.1: Structural drawing of four anthraquinones listed from top to bottom row from left to right. Top row: anthraquinone-2-sulfonic acid ($AQSO_3^-$), anthraquinone-2-carboxylic acid ($AQCO_2H$). Bottom row: anthraquinone-ethanyl-deoxyadenosine phosphate (AQ-E-dA-p), and anthraquinone-ethynyl-deoxyadenosine phosphate (AQ-Y-dA-p). 16

Figure 2.2: Photograph of a CV cell stand (BAS CV-1B): working electrode (WE), auxiliary electrode (AE), reference electrode (RE), stirring controls (switch, and stir rate), gas controls (purge and blanket, and gas rate), and gas lines [blanketing tube (N_2 gas) and purging tube]. 17

Figure 2.3: Photograph of a setup for testing a CV cell: working electrode (WE), auxiliary electrode (AE), reference electrode (RE), N_2 gas lines (blanketing and purging tube). 18

Figure 2.4: CV scan showing how to calculate E_p^a, E_p^c, $E_{1/2}$, and $E_{1/2}$ (SCE). 19

Figure 2.5: CV scan of 0.934 mM FHP in 10 mM phosphate buffer pH 7.0 with 100 mM KCl versus the Ag/AgCl/KCl (sat'd) reference electrode. The X-axis sensitivity was set to 50 mV/cm, Y-axis sensitivity to 2.5 μA/cm, and the scan rate to 100 mV s^{-1}. 20

Figure 2.6: CV scan of 1.01 mM $AQCO_2H$ in 10 mM phosphate buffer pH 7.0 with 100 mM KCl versus the Ag/AgCl/KCl (sat'd) reference electrode. The X-axis sensitivity was set to 50 mV/cm, Y-axis sensitivity to 1.25 μA/cm, and the scan rate to 100 mV s^{-1}. 21

Figure 2.7: CV scan of 0.953 mM AQ-E-dA-p in 10 mM phosphate buffer pH 7.0 with 100 mM KCl versus the Ag/AgCl/KCl (sat'd) reference electrode. The X-axis sensitivity was set to 50 mV/cm, Y-axis sensitivity to 2.5 μA/cm, and the scan rate to 100 mV s^{-1}. 22

Figure 2.8: CV scan of 0.977 mM AQ-Y-dA-p in 10 mM phosphate buffer pH 7.0 with 100 mM KCl versus the Ag/AgCl/KCl (sat'd) reference electrode. The X-axis sensitivity was set to 50 mV/cm, Y-axis sensitivity to 1.25 μA/cm, and the scan rate to 100 mV s^{-1}. 23

Figure 3.1: Anthraquinone indicating the numbering of the substituent position. 40

Figure 3.2: Structures of selected compounds in this study. Full names are given in the List of Abbreviations. 41

Figure 3.3: Structures of anthraquinones studied bearing $COCF_3$ substituents. Full names are given in the List of Abbreviations. 42

Figure 3.4: Structures of selected compounds in this study. Full names are given in the List of Abbreviations. 43

Figure 3.5: Structures of selected compounds in this study. Full names are given in the List of Abbreviations. 44

Figure 3.6: Structures of selected compounds in this study. Full names are given in the List of Abbreviations. 45

Figure 3.7: Structures of selected compounds in this study. Full names are given in the List of Abbreviations. 46

Figure 3.8: Structures of selected compounds in this study. Full names are given in the List of Abbreviations. 47

Figure 4.1: Structures of molecules investigated. 61

Figure 4.2: UV-visible absorbance spectra of AQI 5b as a function of time at room temperature (3:7 MeCN and 60 mM pH = 8.0 borate buffer). Scans were taken every 15 min for the first 2 h and every 1 h for the last 3 h. The absorbance increased at 208 nm and 285 nm, and decreased at 230 nm. 62

Figure 5.1: Anthraquinone-2,3-dimethyl ester structural drawing in Gaussian 03W. 70

Figure 5.2: Electron affinity (eV) versus redox potential values (-V). 71

LIST OF TABLES

Table 2.1: Formula weights, sample weights and concentrations of solutions used for electrochemistry experiments. 24

Table 2.2: BAS CV-27 setting for voltage range, scan speed, and the X-Y recorder setting for X-axis sensitivity and Y-axis sensitivity. 25

Table 2.3: Reference redox potential versus NHE and SCE at 25°C (SCE = NHE – 0.241). 26

Table 2.4: Electrochemical properties of AQ derivatives in 0.101 M KCl in 9.99 mM phosphate buffer, pH 7.01. 27

Table 3.1: Formula weights, sample weights and concentrations of solutions used for electrochemistry experiments. 48

Table 3.2: Electrochemical properties of small AQ derivatives in CH_3CN (V). 49

Table 3.3: Electrochemical properties of AQ nucleosides derivatives CH_3CN (V), reported vs. SCE. 50

Table 3.4: Electrochemical properties of AQ substituent linker series (V). 51

Table 4.1: Reduction potentials of AQ derivatives in acetonitrile (1 mM AQ with 0.1 M TBAH). 63

Table 4.2: Electrochemical properties of AQ diamide and AQ imide derivatives in CH_3CN (V). 64

Table 5.1: Redox potentials, and electron affinity values. 72

Table 5.2: Correlation coefficients for the electron affinity (eV) versus redox potential values (-V) as a function of the substituents excluded. 73

LIST OF ABBREVIATIONS

NaCl	Sodium chloride
HCl	Hydrochloric acid
KCl	Potassium chloride
Ag/AgCl/NaCl (3M)	Silver/silver chloride/sodium chloride
Ag/Ag^+	Silver/silver ion
$AgNO_3$	Silver nitrate
AgO	Silver oxide
N_2	Nitrogen gas
EA	Electron Affinity
CV	Cyclic Voltammetry
DFT	Density Functional Theory
SCE	Saturated Calomel Electrode
TBAH	Tetrabutylammonium hexafluorophosphate
TEAP	Tetraethylammonium perchlorate
CH_3CN	Acetonitrile
ANE2	Ag/Ag^+
Fc	Ferrocene
FHP	Ferrocenium hexafluorophosphate
Al_2O_3	Alumminum oxide
MeOH	Methanol
H_2O	Water
Y	Ethynyl

E	Ethanyl
dA	Deoxyadenosine
dU	Deoxyuracil
TMS	Trimethylsilyl
TDBPS	*tert*-Butyldiphenylsilyl
DMTr	Dimethoxytrityl
AQ	Anthraquinone
AQCN	Anthraquinone-2-carbonitrile
$AQCO_2H$	Anthraquinone-2-carboxylic acid
AQ-2,3-CO_2H	Anthraquinone-2,3-dicarboxylic acid
$AQCO_2CH_3$	Methyl anthraquinone-2-carboxylate
AQ-2,3-CO_2CH_3	Dimethyl anthraquinone-2,3-dicarboxylate
$AQCOCH_3$	2-Acetylanthraquinone
AQCOPh	2-Benzoylanthraquinone
dA-Y-AQ-2,3-CO_2CH_3	Deoxyadenosine-ethynyl-anthraquinone-2,3-dimethyl ester, protected as the TBDPS ether
dA-E-AQ-2,3-CO_2CH_3	Deoxyadenosine-ethanyl-2,3-dimethyl ester, protected as the TBDPS ether
AQI	Anthraquinone-2,3-dicarboximide
AQI-CH_2CCH	*n*-Propargyl-anthraquinone-2,3-dicarboximide
AQI-$CH_2CH_2CH_2OMe$	*N*-(3-Methoxypropyl)-anthraquinone-2,3-dicarboximide
$AQCONHCH_3$	*N*-Methyl-anthraquinone-2-carboxamide

$AQCONHC(CH_3)_3$	*N-tert*-Butyl-anthraquinone-2-carboxamide
$AQCONH(CH_2)_2CH_3$	*N*-Butyl-anthraquinone-2-carboxamide
AQ-E-dA-p	Anthraquinone-ethanyl-deoxyadenosine-phosphate
AQ-Y-dA-p	Anthraquinone-ethynyl-deoxyadenosine-phosphate
AQ-Y-dA	Anthraquinone-ethynyl-deoxyadenosine, protected as the TBDPS ether
AQ-E-dA	Anthraquinone-ethanyl-deoxyadenosine, protected as the TBDPS ether
AQ-Y-dU	Anthraquinone-ethynyl-deoxyuracil, protected as the DMTr ether
dA-Y-$AQCOCF_3$	Deoxyadenosine-ethynyl-2-trifluoroacetyl-anthraquinone, protected as the TBDPS ether
dA-Y-$AQC(OH)_2CF_3$	Deoxyadenosine-ethynyl-2-trifluoroacetyl-anthraquinone dihydrate, protected as the TBDPS ether
$AQSO_3^-$	Anthraquinone-2-sulfonic acid
Y-AQ-2,3-CO_2CH_3	6-Ethynyl-anthraquine-2,3-dimethyl ester
E-AQ-2,3-CO_2CH_3	6-Ethanyl-anthraquine-2,3-dimethyl ester
TMSY-AQ-2,3-CO_2CH_3	Trimethylsilyl-ethynyl-anthraquinone-2,3-dimethyl ester
AQCHO	Anthraquinone-2-carbaldehyde
dA-Y-AQCHO	Deoxyadenosine-ethynyl-anthraquinone-2-carbaldehyde, protected as the TBDPS ether

dA-NHCO-AQ	Deoxyadenosine-anthraquinone-2-carboxamide, protected as the diacetyl derivative
AQ-2,3-CONH$(CH_2)_3OCH_3$	*N,N'*-Bis(3-methoxypropyl)-anthraquinone-2,3-dicarboxamide
AQ-2,3-CONH$(CH_2)_2CH_3$	*N,N'*-Dipropyl-anthraquinone-2,3-dicarboxamide
AQ-8-dU	Anthraquinone-CONHCH_2CH_2NHCOCH=CH-deoxyuracil, protected as the DMTr ether

Chapter 1: Introduction

Electron transfer in DNA has been the focus of extensive studies.[1-10] Some data has been interpreted in terms of DNA being "molecular wire" that allows for long distance charge transport to occur from donor to acceptor.[11-14] Other data have been interpreted in terms of multi-step hopping of the electron (hole) through DNA.

Electron transfer to give a radical cation on DNA usually results in a guanine radical cation. This is because guanine is the most easily oxidized of the four bases.[15,16] Adenine is the second most easily oxidized base, but a recent study that attempted to look at the adenine radical cation found products derived from the thymine radical cation instead presumably because the latter is more reactive and goes quickly to products.[14,17]

Takada et al. were interested in studying the effects of increasing the number of consecutive adenine bases on charge separation.[2] The adenine bases were synthesized in a hairpin DNA conjugates with naphthaldiimide (NDI, electron acceptor) at the 3' end and phenothiazine (electron donor) at the 5' end. The quantum yieldΦ) of the forward reaction decreased from 2.1 x 10^{-2} to 0.65 x 10^{-2} as the chain length increased from 4 to 8 adenines, only a factor of 3.2 for an additional four base pairs. Other sequences studied were those involving only AT bases (ATATATA and ATATATATA) those with both A and G/C bases (AGAGA and AAGAA). The AT sequences had quantum yields of 0.39 x 10^{-2} and 0.13 x 10^{-2}, respectively. The AG/C sequences had quantum yields of 0.37 x 10^{-2} and 0.75 x 10^{-2}, respectively. The consecutive adenine sequences showed higher quantum yields than the AT sequence for the same length, by a factor 3.6 for five bases and 6.5 for seven bases. For the AG/C sequences, adding one and two G/C base pairs reduced the quantum yields by factors of 1.9 and 3.8,

respectively. Thus, charge separation is readily effected over a number of adenines, and is more effective over adenines alone than adenines in combination with any other bases.

Kawai et al. studied the extent of photosensitized DNA damage reactions using naphthalimide (NI) and naphthaldiimide (NDI) derivatives bound and unbound to DNA.[18] Reactions were carried out in phosphate buffer pH 7.0, with 20 μM of NI or NDI derivatives and 25 μM of DNA strands with varying number of consecutive adenines. When either NI or NDI are bound to DNA, adenine is oxidized via the singlet excited state of the imide. When these imides are not bound DNA, the situation is different. NI is only able to oxidize guanine via its triplet excited state, because NI has an redox potential of only -1.01 V versus NHE. In contrast, NDI with an redox potential of -0.22 V, is able to oxidize adenine.[19] The product of the electron transfer is a radical anion.[18] $NDI^{\bullet-}$ has a slower rate of reaction with molecular oxygen (4.2×10^{7} M^{-1} s^{-1}) than does $NI^{\bullet-}$ (1.2×10^{9} M^{-1} s^{-1}), allowing longer lived charge separated species in the former case. It was observed, as expected, that more DNA damage was found with NDI than with NI. It was also expected that NI and NDI bound to DNA would give greater amount of DNA damage than unbound to DNA (i.e., derivatives with a net negative charge). However, this was not observed. NDIP unbound to DNA yielded the greatest amount of DNA damage, while NIP bound to DNA yielded only moderate damage to DNA. For all of the derivatives, the unbound compound caused more damage than the bound compound.

To study adenine oxidation in DNA, new approaches are needed. One approach is to covalently attach an electron acceptor to the adenine. Photolysis might then give the adenine radical cation – acceptor radical anion pair. The reaction will be aided by a high driving force, which may be achieved by changes in the reduction potential of the acceptor.

Anthraquinones are widely used in DNA electron transfer studies.[11,17,20-23] The anthraquinone excited singlet state (n,π) can efficiently undergo intersystem crossing to the triple state (π,π) in less than 50 ps.[22] When anthraquinone is in its excited state, it can accept an electron from the adjacent base creating a radical ion pair.[11] The AQ radical anion can be quenched by oxygen to form superoxide. Hussein et al. have shown that the radical cation of deoxyadenosine can form upon photolysis of an anthraquinone-dA conjugate; the radical cation has moderate absorption from 400 to 600 nm.[22] In CH_3CN, the charge transfer state for anthraquinone anion – deoxyadenosine radical cation had a lifetime of 2.2 ns.

Gorodetsky et al. studied anthraquinones attached to DNA through alkane and ethynyl linkers.[24] Anthraquinone itself was attached either to uracil via an ethynyl linker or to the 5'-end of the DNA chain through a $(CH_2)_6$ linker. These conjugates were studied using square wave and cyclic voltammetry on gold electrodes. The alkane and alkyne conjugates had redox potentials (versus NHE) of -0.330 ± 0.060 V and -0.301 ± 0.007 V, respectively. Thus, these two conjugates have the same redox potential within experimental error. The ethynyl conjugate had a higher current (160 ± 50 nA) than the alkane linker (9 ± 4 nA).

The goal of the study was to create a series of anthraquinones with electron-withdrawing groups to enhance the probability of electron transfer occurring in DNA. It was particularly important to make AQ-dA conjugates if electron transfer is to be studied in DNA itself, rather than only in model systems. In this thesis, reduction potentials are reported for a series of anthraquinones and anthraquinone conjugates. In addition, calculations of the electron affinities of these species are reported and correlated with experimental observations.

1.1 References

1. Takada, T.; Kawai, K.; Fujitsuka, M.; Majima, T. Rapid long-distance hole transfer through consecutive adenine sequence *J. Am. Chem. Soc.* **2006**, *128*, 11012-11013.

2. Takada, T.; Kawai, K.; Cai, X. C.; Sugimoto, A.; Fujitsuka, M.; Majima, T. Charge separation in DNA via consecutive adenine hopping *J. Am. Chem. Soc.* **2004**, *126*, 1125-1129.

3. Nordlund, T. M. Sequence, structure and energy transfer in DNA *Photochem. Photobiol.* **2007**, *83*, 625-636.

4. Nogues, C.; Cohen, S. R.; Daube, S.; Apter, N.; Naaman, R. Sequence dependence of charge transport properties of DNA *J. Phys. Chem. B* **2006**, *110*, 8910-8913.

5. Bixon, M.; Jortner, J. Long-range and very long-range charge transport in DNA *J. Phys. Chem.* **2002**, *281*, 393-408.

6. Giese, B.; Amaudrut, J.; Kohler, A. K.; Spormann, M.; Wessely, S. Direct observation of hole transfer through DNA by hopping between adenine bases and by tunnelling *Nature* **2001**, *412*, 318-320.

7. Kawai, K.; Takada, T.; Tojo, S.; Majima, T. Kinetics of weak distance-dependent hole transfer in DNA by adenine-hopping mechanism *J. Am. Chem. Soc.* **2003**, *125*, 6842-6843.

8. Takada, T.; Kawai, K.; Fujitsuka, M.; Majima, T. High-yield generation of a long-lived charge-separated state in diphenylacetylene-modified DNA *Angew. Chem. Int. Ed.* **2006**, *45*, 120-122.

9. Augustyn, K. E.; Genereux, J. C.; Barton, J. K. Distance-independent DNA charge transport across an adenine tract *Angew. Chem. Int. Ed.* **2007**, *46*, 5731-5733.

10. Liu, T.; Barton, J. K. DNA electrochemistry through the base pairs not the sugar-phosphate backbone *J. Am. Chem. Soc.* **2005**, *127*, 10160-10161.

11. Joy, A.; Schuster, G. B. Long-range radical cation migration in DNA: Investigation of the mechanism *Chem. Commun.* **2005**, 2778-2784.

12. Murphy, C. J.; Arkin, M. R.; Jenkins, Y.; Ghatlia, N. D.; Bossmann, S. H.; Turro, N. J.; Barton, J. K. Long-range photoinduced electron-transfer through a DNA helix *Science* **1993**, *262*, 1025-1029.

13. Jortner, J.; Bixon, M.; Langenbacher, T.; Michel-Beyerle, M. E. Charge transfer and transport in DNA *Proc. Natl. Acad. Sci. U. S. A.* **1998**, *95*, 12759-12765.

14. Ghosh, A.; Joy, A.; Schuster, G. B.; Douki, T.; Cadet, J. Selective one-electron oxidation of duplex DNA oligomers: Reaction at thymines *Org. Biomol. Chem.* **2008**, *6*, 916-928.

15. Giese, B. Long distance charge transport in DNA: The hopping mechanism *Acc. Chem. Res.* **2000**, *33*, 631-636.

16. Douki, T.; Cadet, J. Modification of DNA bases by photosensitized one-electron oxidation *Int. J. Radiat. Biol.* **1999**, *75*, 571-581.

17. Joy, A.; Ghosh, A. K.; Schuster, G. B. One-electron oxidation of DNA oligomers that lack guanine: Reaction and strand cleavage at remote thymines by long-distance radical cation hopping *J. Am. Chem. Soc.* **2006**, *128*, 5346-5347.

18. Kawai, K.; Osakada, Y.; Fujitsuka, M.; Majima, T. Hole transfer in DNA and photosensitized DNA damage: Importance of adenine oxidation *J. Phys. Chem. B* **2007**, *111*, 2322-2326.

19. Rogers, J. E.; Kelly, L. A. Nucleic acid oxidation mediated by naphthalene and benzophenone imide and diimide derivatives: Consequences for DNA redox chemistry *J. Am. Chem. Soc.* 1999, *121*, 3854-3861.

20. Shao, F. W.; Augustyn, K.; Barton, J. K. Sequence dependence of charge transport through DNA domains *J. Am. Chem. Soc.* **2005**, *127*, 17445-17452.

21. Tanabe, K.; Iida, H.; Haruna, K. I.; Kamei, T.; Okamoto, A.; Nishimoto, S. I. Electrochemical evaluation of alternating duplex-triplex conversion effect on the anthraquinone-photoinjected hole transport through DNA duplex immobilized on a gold electrode *J. Am. Chem. Soc.* **2006**, *128*, 692-693.

22. Hussein, Y. H. A.; Anderson, N.; Lian, T. T.; Abdou, I. M.; Strekowski, L.; Timoshchuk, V. A.; Vaghefi, M. M.; Netzel, T. L. Solvent and linker influences on $AQ^{-}/dA^{\cdot+}$ charge-transfer state energetics and dynamics in anthraquinonyl-linker-deoxyadenosine conjugates *J. Phys. Chem. A* **2006**, *110*, 4320-4328.

23. Tierney, M. T.; Grinstaff, M. W. Synthesis and stability of oligodeoxynucleotides containing c8-labeled 2 '-deoxyadenosine: Novel redox nucleobase probes for DNA-mediated charge-transfer studies *Org. Lett.* **2000**, *2*, 3413-3416.

24. Gorodetsky, A. A.; Green, O.; Yavin, E.; Barton, J. K. Coupling into the base pair stack is necessary for DNA-mediated electrochemistry *Bioconjug. Chem.* **2007**, *18*, 1434-1441.

Chapter 2: The Experimental Protocol

2.0 Introduction

Our long term goal is to study electron-transfer in systems in which anthraquinone is covalently linked to DNA.[1-14] The specific overall goal of the current study was to compare the effect of the linker (ethanyl or ethynyl) on the reduction potential of the anthraquinone deoxyadenosine conjugate.

This chapter describes the experimental protocol for the cyclic voltammetry studies. Cyclic voltammetry is a potentiostat method involving an electronic device that controls the potentials of the working electrode.[15] The working electrode has a potential that is varied linearly with time. The reference redox potential is kept constant throughout the entire experiment. The auxiliary electrode conducts electricity from the electron device through to the solution to the working electrode. The Nernst equation is used to calculate equilibrium reduction potentials. The Nernst equation is $E = E° - (RT/zF)* \ln(red/ox)$, where E° is the standard redox potential, R is the universal gas constant, and T is the absolute temperature, F is the Faraday constant, and z is the number of electrons transferred in the reaction.[15]

We verified the cyclic voltammetry protocol by measuring the reduction potential of $AQSO_3^-$ as this value has previously been measured in H_2O.[16-19] We also measured the reduction potential of $AQCO_2H$ in water.[20] Finally, we measured the redox potential of AQ bound to deoxyadenosine via ethanyl (AQ-E-dA-p) and ethynyl (AQ-Y-dA-p) linkers.

2.1 Materials and Methods

Potassium chloride (Baker Analyzed, Phillipsburg, NJ), sodium phosphate dibasic (Aldrich, Milwaukee, WI), and hydrochloric acid (Baker Analyzed, Phillipsburg, NJ) were

purchased from the indicated suppliers. All aqueous solutions were prepared in 18.6 MΩ-cm water from a Milli-Q water purification system (Millipore).

2.1.1 Preparation of Solutions

The phosphate buffer was prepared by dissolving 0.709 g of sodium phosphate dibasic (Aldrich) in 500 mL of water, yielding a buffer 9.99 mM in phosphate. The pH of the phosphate buffer was adjusted from 9.17 to 7.01 by adding 1.0 M HCl. The buffer was stored at 4 ^{o}C.

Sodium chloride (Aldrich) solution was prepared by dissolving 0.584 g NaCl in 10 mL of phosphate buffer pH 7.01, yielding 0.999 M. The solution was stored at 4 ^{o}C.

Ferrocenium hexafluorophosphate (71%, Aldrich, Milwaukee, WI) solution was prepared by dissolving 4.44 mg in 10 mL of 0.999 M NaCl phosphate buffer pH 7.01. The ferrocenium hexafluorophosphate did not fully dissolve, and the solution was filtered using a syringe and a Nalgene filter (surfactant-free cellulose acetate, 0.2 μm, 25 mm).

A saturated potassium chloride solution was prepared by dissolving 3.548 g KCl in 10 mL water, yielding a 4.76 M solution (10% beyond the KCl saturation limit). The solution was left stirring overnight with Parafilm cover.

KCl (0.750 g) was dissolved in 100 mL of 9.99 mM phosphate buffer pH 7.01 yielding a 0.101 M solution.

2.1.2 The Procedure for Making Ag/AgCl/Cl^- Reference Electrode

The Ag/AgCl/NaCl (3 M) reference electrode was purchased from BASi, Inc (Lafayette, IN). The necessary steps were taken to change the 3 M NaCl solution to a KCl (sat'd) solution. The yellow polymer that sealed the VYCOR frit was cut, being careful not to touch the Ag/AgCl wire (the Ag region of the wire is shiny near the top). The heat shrink tubing was cut and the VYCOR frit was discarded. The NaCl solution was extracted using a syringe. The electrode

body was washed with water four times, and then dried with nitrogen gas. A saturated KCl solution was added to the electrode tube, so that the salt solution touched the shiny portion of the Ag-region at the top. The VYCOR frit was replaced by using a heat gun on low heat. The electrode was held in between two fingers just below the heat shrink tubing with the frit pointing upward and rotating the tubing in the hot air flow for 30 sec. It was only required that 40% of the VYCOR frit be covered by the tubing. The frit was wetted by placing the electrode in the saturated KCl solution. The storage tube was capped and sealed with Parafilm.

2.1.3 The Procedure for Polishing the Working Electrode

The working electrode (glassy carbon) was polished with alumina powder (0.05 μm, Buehler, Lake Bluff, IL) for 30 seconds on a CRYSTALMASTER 6 PLUS (Abrasive Technology, Lewis Center, OH), and sonicated in Branson 2200 Sonicator for 10 min in MeOH:H_2O (1:1 v/v). They were dried with a Kimwipe and N_2 gas and used to record two scans. The electrode was cleaned after every second scan.

2.1.4 The Procedure for Cleaning the Auxiliary Electrode

The auxiliary electrode was cleaned with lens paper and a small amount of methanol by rubbing the lens paper against the platinum wire.

2.1.5 Preparation of Anthraquinones in Aqueous Solutions

Anthraquinone-2-sulfonic acid ($AQSO_3^-$, 97%, Aldrich, Milwaukee, WI), and anthraquinone-2-carboxylic acid ($AQCO_2H$, TCI America, Portland, OR) (Figure 2.1) were used as received. Anthraquinone-ethanyl-deoxyadenosine phosphate (AQ-E-dA-p) and anthraquinone-ethynyl-deoxyadenosine phosphate (AQ-Y-dA-p) (Figure 2.1) were gifts of Reham Abou-Elkhair. The compounds were prepared for use as indicated in Table 2.1.

2.2 Cyclic Voltammograph

The electrochemical system includes a BAS CV-27 voltammograph, a BAS C-1B cell stand (Figure 2.2), a CV cell (Figure 2.3), and a BAS XY analog recorder. The BAS CV-27 voltage and current ranges were set to ± 0.5 V, and ± 50 mA, respectively. The current sensitivity or gain was set to 0.2 mA/V and the scan speed was set to 100 mV/s. One side of a 10 kΩ resistor was connected to the reference/auxiliary electrode circuits, and the other side was connected to the working electrode circuit. Eight voltages were set manually in the ± 0.5 V range and the currents (μA) that passed through the resistor recorded. In every case the current was equal to V/R (for example, 23 μA = 0.23 V/10 kΩ).

2.2.1 Applying Electrochemistry for Aqueous Solution

For all H_2O experiments, the solution was purged and stirred with 30 min with N_2 gas. The BAS-CV27 was set up with a three-electrode system: the reference electrode was Ag/AgCl/KCl (sat'd), the auxiliary electrode was platinum, and the working electrode was gold. Ferrocenium hexafluorophosphate was measured first with a voltage range of 0.80 to -0.20V, X-axis sensitivity at 50 mV/cm, Y-axis sensitivity at 2.5 μA/cm, and scan speed at 100 mV/cm (Figure 2.4). Table 2.2 reports the scan range, X- and Y-axis sensitivities and scan speeds.

2.2.2 Confirming the XY Recorder was Working Properly

The analog recorder plotted voltages on x- and y-axes. The x-axis sensitivity was set to 50 mV/cm resulting in a pen range of 20 cm [= 2 x 0.5 V/(50 mV/cm)]. The y-axis sensitivity was also set to 50 mV/cm and the CV-27 sensitivity was set to 0.2 mA/V. The product of these two settings yielded an overall plotter response to the electrochemical current of 10 μA/cm (= 0.2 mA/V x 50 mV/cm). Thus, one centimeter of y-axis recorder movement signaled 10 μA of electrochemical current in the resistor (or eventually the cell). For the 10 kΩ resistor test, the

observed current range was ± 50 μA (± 0.5 V/10 kΩ). This produced 10 cm of y-axis chart displacement [= 2 x 50 μA/(10 μA/cm)].

2.2.3 Calculating Redox Potentials from CV

Before the cyclic voltammetry scan began, a vertical line was drawn using an ink pen. A cyclic voltammogram was taped to a drawing board and aligned with a T-square. Using a ruler, a line was drawn as close as possible to the top and bottom of the cathodic and anodic peaks. A perpendicular line was drawn at the point where the line no longer slopes. Using a centimeter ruler, the zero mark was placed in the middle of the black line drawn by the pen, and the anodic and cathodic peak were measured. Once the distances of the anodic and cathodic peaks were measured, the redox potentials were calculated by multiplying the x-axis sensitivity by the distance and having it subtracted from the initial voltage applied (Figure 2.5). The redox potential was then calculated by taking the average of the anodic and cathodic peaks versus the electrode used. In H_2O solution, to convert $E_{½}$ Ag/AgCl/KCl (sat'd) reference electrode into $E_{½}$ vs. SCE, SCE = $E_{½}$(sat KCl) – 0.045 V.[21]

2.2.4 Ferrocenium Hexafluorophosphate and the Ag/AgCl/NaCl (3 M) Reference Electrode

The Ag/AgCl/KCl (sat'd) reference electrode was converted into SCE by subtracting 0.045 mV from the resulting redox potential from cyclic voltammetry data. The electrode can be stored and used for up to one year, as long as it has not dried out or no salt has participated.

2.3 Results and Discussion

2.3.1 Selection of Electrode

There are three types of aqueous electrodes, 3 M NaCl, NaCl (sat'd solution), and KCl (sat'd solution). Each electrode produces a specific redox potential value at 25°C. We used a KCl (sat'd) electrode, primarily due to the popularity of the electrode in laboratory research. The

electrodes (Ag/AgCl) purchased from BASi, Inc. were delivered with 3 M NaCl solution; these were converted to KCl (sat'd) solution. Table 2.3 gives the relationship between the electrode and the correction used to establish redox potential versus SCE or NHE.

An initial run with ferrocenium hexafluorophosphate gave a value of 0.200 V, identical to that previously found in our laboratory (Yasser Hussein, Georgia State University).

2.3.2 Reduction of Anthraquinone

The voltammograms were recorded with a glassy carbon working electrode from 0.80 to -1.60 V with a constant scan rate 100 mV/S. $AQSO_3^-$, $AQCO_2H$ (Figure 2.6), AQ-E-dA-p (Figure 2.7), and AQ-Y-dA-p (Figure 2.8) cyclic voltammograms gave anodic and cathodic peak values. Table 2.4 gives the anodic and cathodic peak potentials, Δ peak potentials, and the half wave reduction potentials ($E_{½}$). The $E_{½}$ was calculated by averaging the anodic and cathodic peaks.

$AQSO_3^-$ in 0.1 M KCl was measured using an Ag/AgCl/KCl (sat'd) reference electrode; an redox potential of -0.602 V vs. SCE was recorded. A literature study reported that the redox potential of $AQSO_3^-$ in sodium hydroxide using an Ag/AgCl/KCl (3 M) reference electrode was -0.620 V.[18] Thus, the difference in these two measurements was 18 mV; this may be due to the difference in electrolytes (phosphate buffer pH 7.01 and NaOH solution). Other literature references do not allow direct comparison as either the electrode or analyte were not specified or the analyte was not ionic.[16,17,19]

$AQCO_2H$ in 0.1 M KCl with Ag/AgCl/KCl (sat'd) reference electrode gave an redox potential of -0.647 V. A literature study gave a value -0.480 V for the redox potential of $AQCO_2H$ in 0.2 M KCl in a phosphate buffer pH 7.0 with an Ag/AgCl/KCl (1 M) reference electrode.[20] Assuming that this was reported vs. NHE, and therefore that the standard correction

of -0.242 V should be applied, the value would be -0.735 V. If this is correct, there was a significant difference in the redox potential of 0.088 V for $AQCO_2H$ in 0.1 M KCl versus 0.2 M KCl solution.

The AQ-E-dA-p and AQ-Y-dA-p were studied. The redox potential values were -0.543 V and -0.510 V, respectively. Thus, there was almost no difference in the reduction potentials as a function of linker (ethanyl vs. ethynyl) for the AQ conjugated dA.

2.4 References

1. Kumamoto, S.; Watanabe, M.; Kawakami, N.; Nakamura, M.; Yamana, K. 2'-Anthraquinone-conjugated oligonucleotide as an electrochemical probe for DNA mismatch *Bioconjugate Chem.* **2008**, *19*, 65-69.

2. Loeff, I.; Rabani, J.; Treinin, A.; Linschitz, H. Charge-transfer and reactivity of n,π* and π,π* organic triplets, including anthraquinonesulfonates, in interactions with inorganic anions: A comparative-study based on classical Marcus theory *J. Am. Chem. Soc.* **1993**, *115*, 8933-8942.

3. Whittemore, N. A.; Mullenix, A. N.; Inamati, G. B.; Manoharan, M.; Cook, P. D.; Tuinman, A. A.; Baker, D. C.; Chambers, J. Q. Synthesis and electrochemistry of anthraquinone-oligodeoxynucleotide conjugates *Bioconjugate Chem.* **1999**, *10*, 261-270.

4. Huang, E.; Zhou, F.; Deng, L. Studies of surface coverage and orientation of DNA molecules immobilized onto preformed alkanethiol self-assembled monolayers *Langmuir* **2000**, 16, 3272-3280.

5. Kertesz, V.; Whittemore, N. A.; Chambers, J. Q.; McKinney, M. S.; Baker, D. C. Surface titration of DNA-modified gold electrodes with a thiol-tethered anthraquinone *J. Electroanal. Chem.* **2000**, *493*, 28-36.

6. Liu, Y.; Hu, N. Loading/release behavior of (chitosan/DNA)$_n$ layer-by-layer films toward negatively charged anthraquinone and its application in electrochemical detection of natural DNA damage *Biosens. Bioelectron.* **2007**, *23*, 661-667.

7. Mbindyo, J.; Zhou, L.; Zhang, Z.; Stuart, J. D.; Rusling, J. F. Detection of chemically induced DNA damage by derivative square wave voltammetry *Anal. Chem.* **2000**, 72, 2059-2065.

8. Wong, E. L. S.; Mearns, F. J.; Gooding, J. J. Further development of an electrochemical DNA hybridization biosensor based on long-range electron transfer *Sens. Actuators, B* **2005**, *111-112*, 515-521.

9. Kamal, A.; Ramu, R.; Tekumalla, V.; Khanna, G. B. R.; Barkume, M. S.; Juvekar, A. S.; Zingde, S. M. Synthesis, DNA binding, and cytotoxicity studies of pyrrolo[2,1-c][1,4]benzodiazepine-anthraquinone conjugates *Bioorg. Med. Chem.* **2007**, *15*, 6868-6875.

10. Gorodetsky, A. A.; Green, O.; Yavin, E.; Barton, J. K. Coupling into the base pair stack is necessary for DNA-mediated electrochemistry *Bioconjugate Chem.* **2007**, *18*, 1434-1441.

11. Abou-Elkhair, R. A. I.; Netzel, T. L. Synthesis of two 8-[(anthraquinone-2-yl)-linked]-2'-deoxyadenosine 3'-benzyl hydrogen phosphates for studies of photoinduced hole transport in DNA *Nucleosides Nucleotides & Nucleic Acids* **2005**, *24*, 85-110.

12. Boon, E. M.; Barton, J. K. Charge transport in DNA *Curr. Opin. Struct. Biol.* **2002**, *12*, 320-329.

13. Di Giusto, D. A.; Wlassoff, W. A.; Giesebrecht, S.; Gooding, J. J.; King, G. C. Enzymatic synthesis of redox-labeled RNA and dual-potential detection at DNA-modified electrodes *Angew. Chem. Int. Ed.* **2004**, *43*, 2809-2812.

14. Yamana, K.; Kumamoto, S.; Nakano, H.; Sugie, Y. Electrochemistry of DNA duplex containing an anthraquinonylmethyl group at the 2'-sugar position *Nucleic Acids Res Suppl* **2001**, 35-36.

15. Skoog, D. A.; Holler, F. J.; Nieman, T. A. *Principles of Instrumental Analysis*; Brooks/Cole Thomson Learning: Clifton Park, **1998**, 570-641.

16. Sheng, Z. Z. Steady-state and laser flash photolysis studies on the oxidative splitting of cyclobutane thymine dimer by triplet 9,10-anthraquinone-2-sulfonate *J. Photochem. Photobiol. A* **2004**, *161*, 99-104.

17. Pandey, P. Application of photochemical-reaction in electrochemical detection of DNA intercalation *Anal. Chem.* **1994**, *66*, 1236-1241.

18. Bechtold, T. Anthraquinones as mediators for the indirect cathodic reduction of dispersed organic dyestuffs *J. Electroanal. Chem. Interfacial Electrochem.* **1999**, *465*, 80-87.

19. Shoute, L. Pulse radiolysis study of one-electron reduction reaction of fluoranil in aqueous solution *J. Phys. Chem.* **1994**, *98*, 11094-11098.

20. Mogharrab, N.; Ghourchian, H. Anthraquinone 2-carboxylic acid as an electron shuttling mediator and attached electron relay for horseradish peroxidase *Electrochem. Commun.* **2005**, *7*, 466-471.

21. Bard, A. J.; Faulkner, L.R. *Electrochemical Methods: Fundamentals and Applications* John Wiley & Sons, Inc: Hoboken, **2001**, 62.

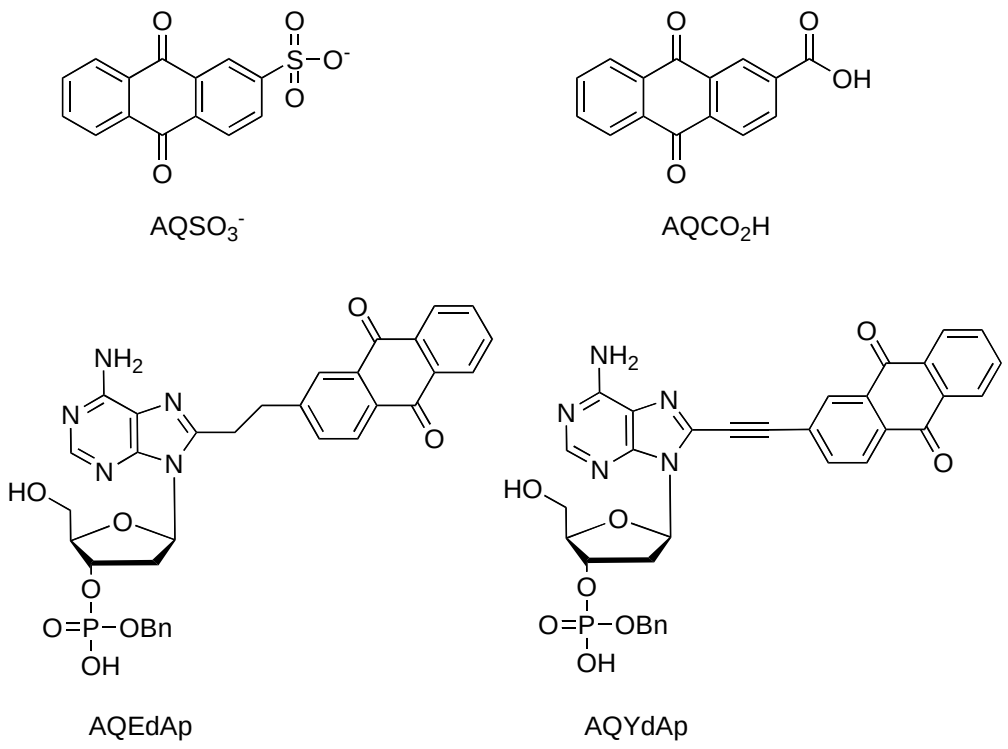

Figure 2.1: Structural drawing of four anthraquinones listed from top to bottom row from left to right. Top row: anthraquinone-2-sulfonic acid ($AQSO_3^-$), anthraquinone-2-carboxylic acid ($AQCO_2H$). Bottom row: anthraquinone-ethanyl-deoxyadenosine phosphate (AQ-E-dA-p), and anthraquinone-ethynyl-deoxyadenosine phosphate (AQ-Y-dA-p).

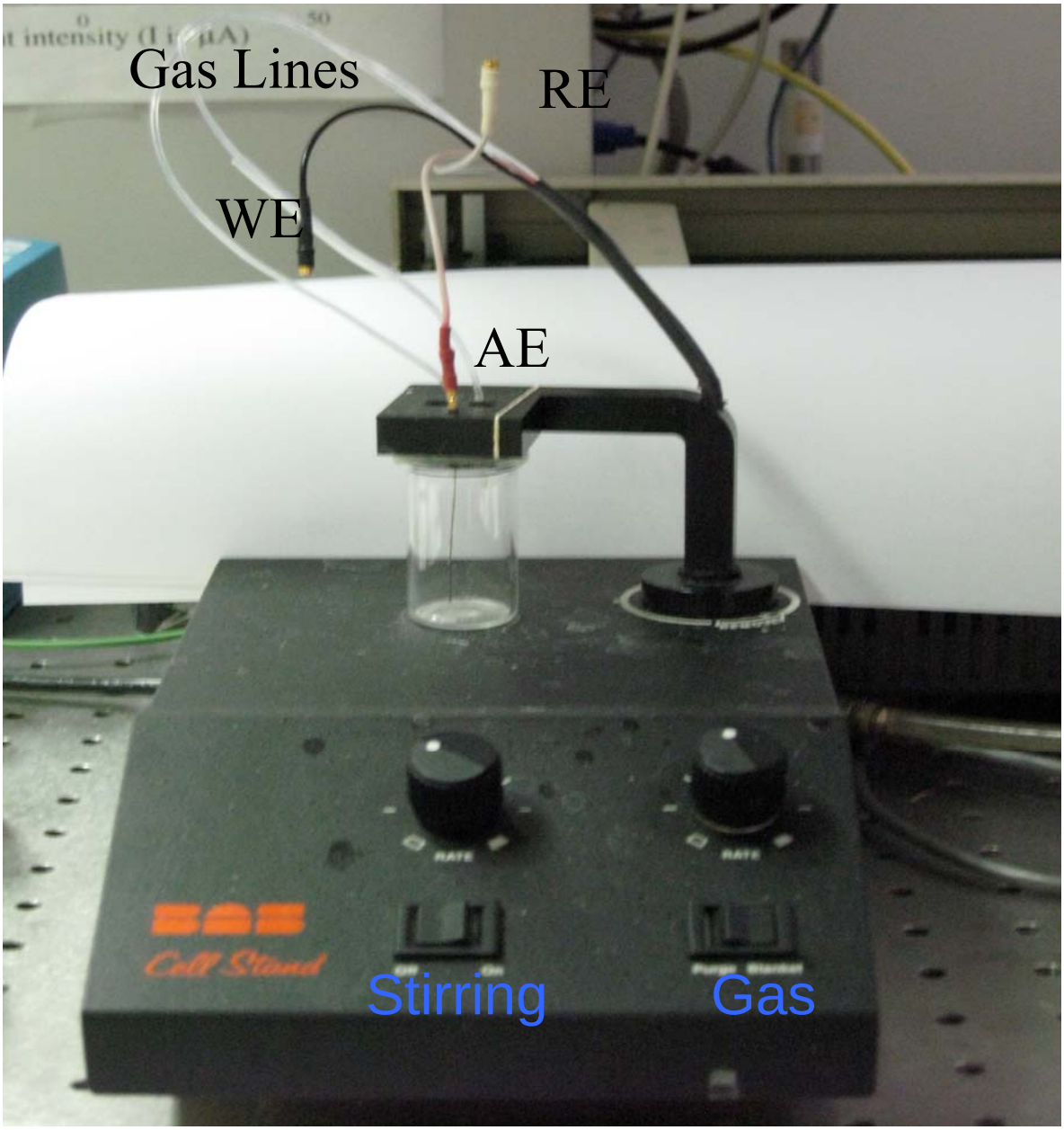

Figure 2.2: Photograph of a CV cell stand (BAS CV-1B): working electrode (WE), auxiliary electrode (AE), reference electrode (RE), stirring controls (switch, and stir rate), gas controls (purge and blanket, and gas rate), and gas lines [blanketing tube (N_2 gas) and purging tube].

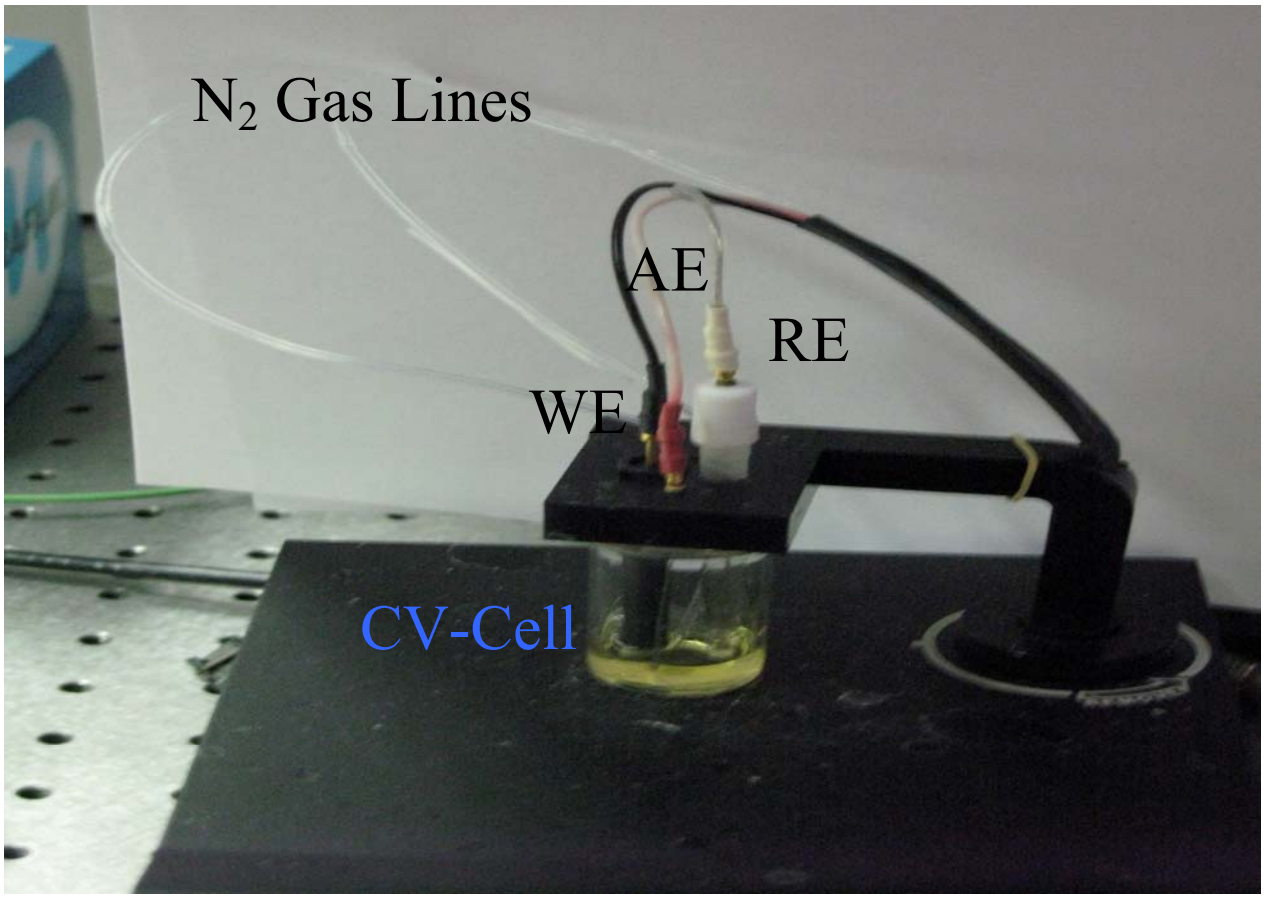

Figure 2.3: Photograph of a setup for testing a CV cell: working electrode (WE), auxiliary electrode (AE), reference electrode (RE), N_2 gas lines (blanketing and purging tube).

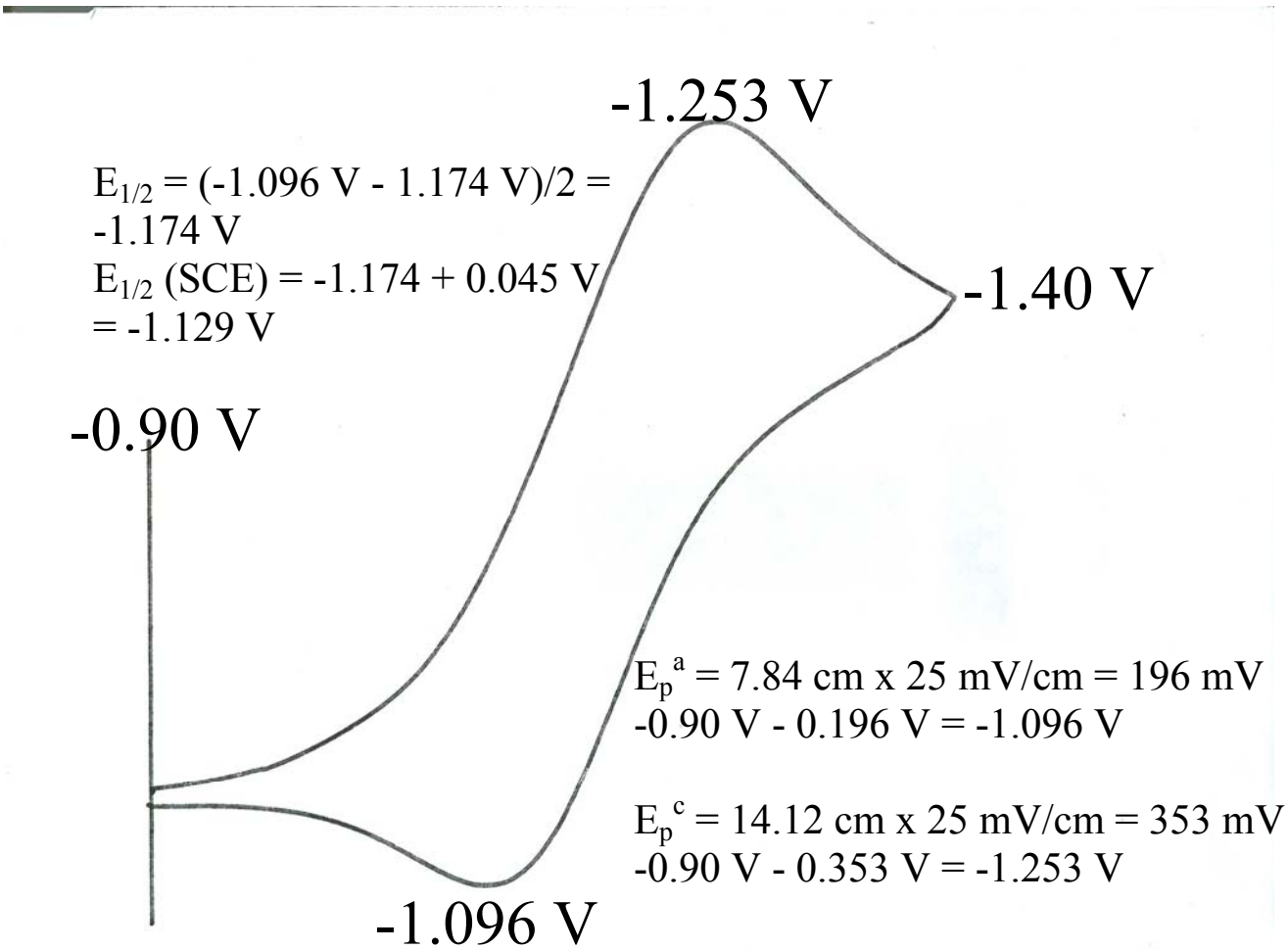

Figure 2.4: CV scan showing how to calculate E_p^a, E_p^c, $E_{1/2}$, and $E_{1/2}$ (SCE).

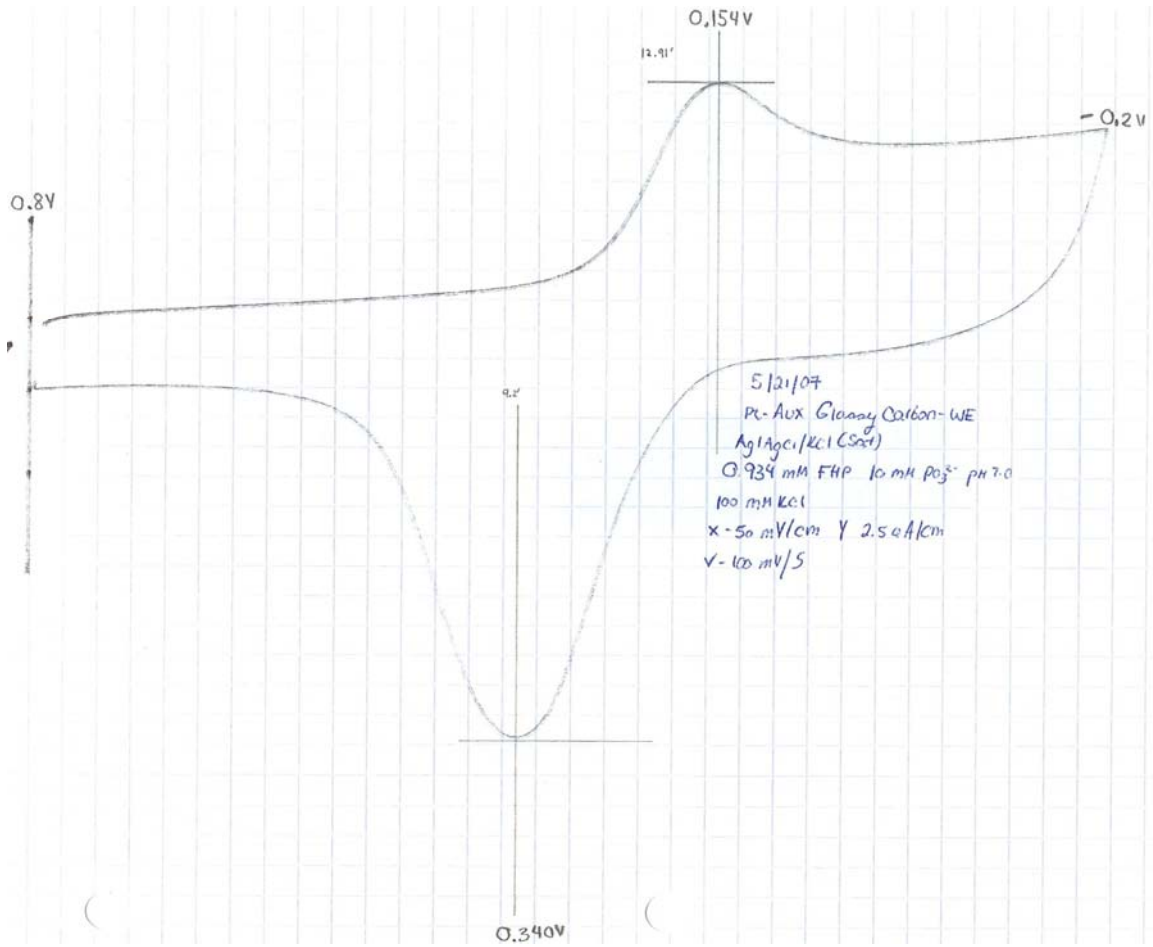

Figure 2.5: CV scan of 0.934 mM FHP in 10 mM phosphate buffer pH 7.0 with 100 mM KCl versus the Ag/AgCl/KCl (sat'd) reference electrode. The X-axis sensitivity was set to 50 mV/cm, Y-axis sensitivity to 2.5 µA/cm, and the scan rate to 100 mV s^{-1}.

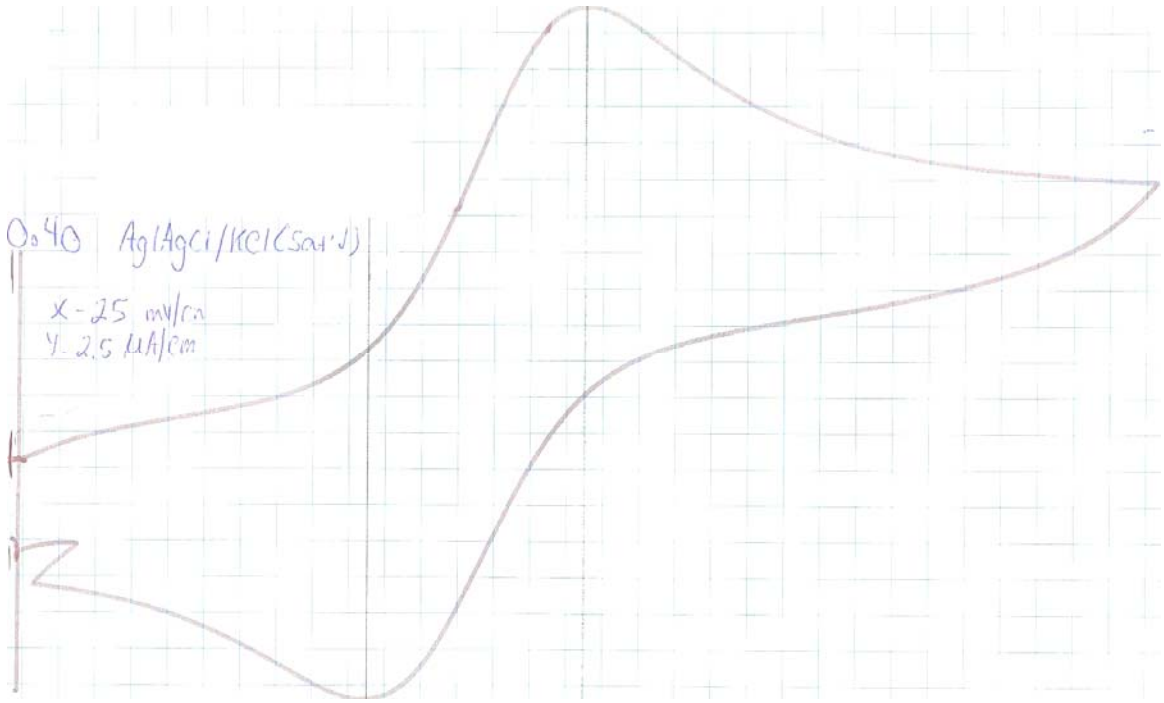

Figure 2.6: CV scan of 1.01 mM $AQCO_2H$ 1.01 mM in 10 mM phosphate buffer pH 7.0 with 100 mM KCl versus the Ag/AgCl/KCl (sat'd) reference electrode. The X-axis sensitivity was set to 50 mV/cm, Y-axis sensitivity to 1.25 μA/cm, and the scan rate to 100 mV s^{-1}.

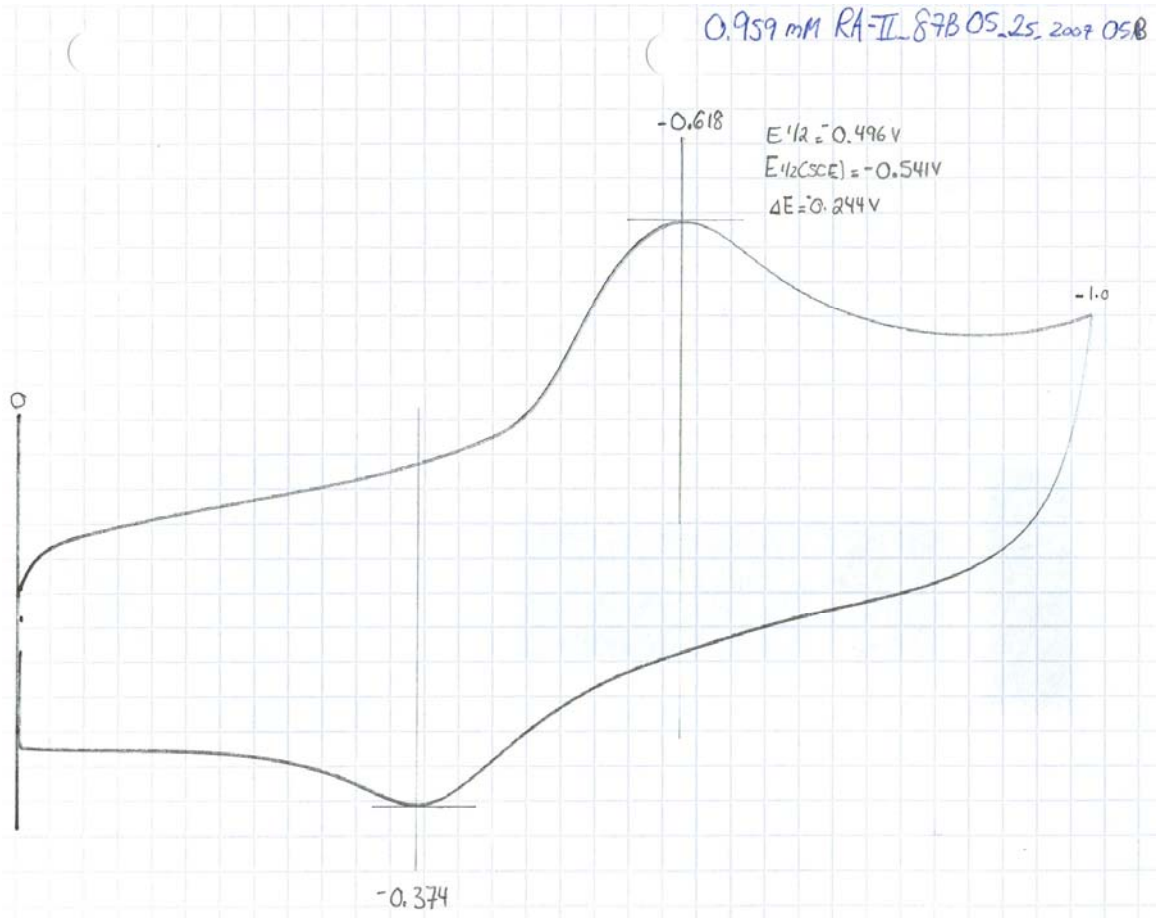

Figure 2.7: CV scan of 0.953 mM AQ-E-dA-p in 10 mM phosphate buffer pH 7.0 with 100 mM KCl versus the Ag/AgCl/KCl (sat'd) reference electrode. The X-axis sensitivity was set to 50 mV/cm, Y-axis sensitivity to 2.5 μA/cm, and the scan rate to 100 mV s^{-1}.

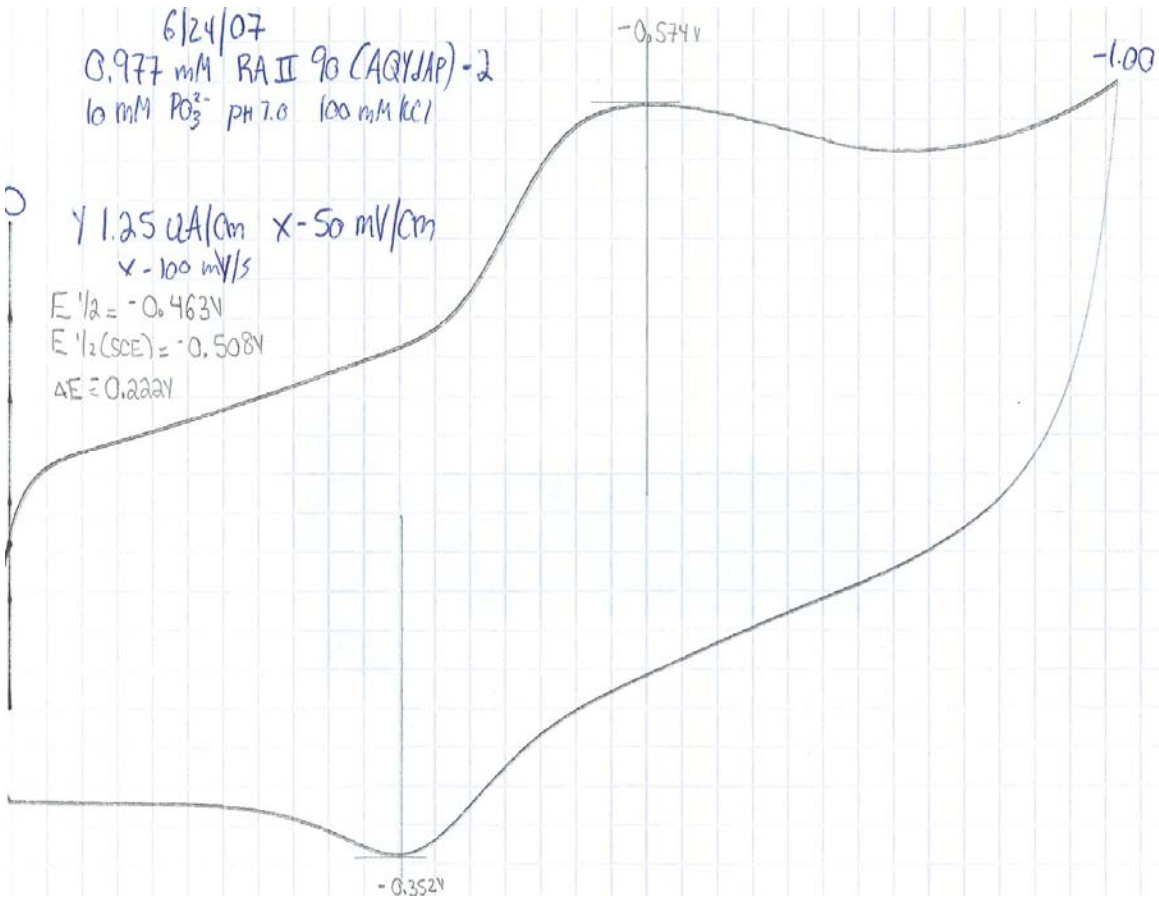

Figure 2.8: CV scan of 0.977 mM AQ-Y-dA-p in 10 mM phosphate buffer pH 7.0 with 100 mM KCl versus the Ag/AgCl/KCl (sat'd) reference electrode. The X-axis sensitivity was set to 50 mV/cm, Y-axis sensitivity to 1.25 µA/cm, and the scan rate to 100 mV s^{-1}.

Table 2.1: Formula weights, sample weights and concentrations of solutions used for electrochemistry experiments.

Sample	Conc (mM)	F.W. (g/mol)	Mass (mg)	10 mM phosphate buffer in 0.1 M KCl, pH 7.0 (mL)
Ferrocene hexafluorophosphate	1.22	331.00	4.83	12.0
Anthraquinone-2-sulfonic acid	0.899	328.28	2.95	10.0
Anthraquinone-2,3-carboxylic acid	1.01	296.23	2.98	10.0
Anthraquinone-E-dA phosphate	0.95	655.59	5.0	8.0
Anthraquinone-Y-dA phosphate	0.98	651.56	7.0	11.0

Table 2.2: BAS CV-27 setting for voltage range, scan speed, and the X-Y recorder settings for X-axis sensitivity and Y-axis sensitivity.

Sample	Scan range (V)	X-axis (mV/cm)	Y-axis (μA/cm)	Scan speed (mV/s)
FHP	0.80 to -0.20	50	2.50	100
$AQSO_3^-$	-0.20 to -0.80	25	1.25	100
$AQCO_2H$	-0.40 to -0.90	50	2.50	100
AQ-E-dA-p	0.00 to -1.00	50	1.25	100
AQ-Y-dA-p	0.00 to -1.00	50	1.25	100

Table 2.3: Reference redox potential versus NHE and SCE at 25°C (SCE = NHE – 0.241).

Aqueous solution	Potential vs. NHE	Potential vs. SCE
Ag/AgCl/NaCl (3 M)	0.206	-0.035
Ag/AgCl/NaCl (sat'd)	0.194	-0.047
Ag/AgCl/KCl (sat'd)	0.196	-0.045
Ag/AgCl/KCl (3 M)	0.210	-0.032

Table 2.4: Electrochemical properties of AQ derivatives in 0.101 M KCl in 9.99 mM phosphate buffer, pH 7.01.

Compound	E_p^a (V)	E_p^c (V)	ΔE (V)	$E_{½}$ (SCE) (V)[a]
$AQSO_3^-$	-0.526	-0.588	0.062	-0.602
$AQCO_2H$	-0.553	-0.648	0.085	-0.647
AQ-E-dA-p	-0.374	-0.627	0.253	-0.543 ± 0.002
AQ-Y-dA-p	-0.570	-0.359	0.211	-0.510 ± 0.003

[a] The data for the $AQSO_3^-$ and $AQCO_2H$ were single scans, and AQ-E-dA-p and AQ-Y-dA-p are average of 3 scans.

Chapter 3: Study of Substituted Anthraquinones in CH_3CN

3.0 Introduction

Ferrocene (Fc) is commonly used as internal standard in non-aqueous solvents.[1-9] Ferrocene has an redox potential of 0.087 V in the ANE2 electrode, which consists of tetraethylammonium perchlorate (TEAP) in 0.01 M acetonitrile (CH_3CN).[2] The current study used tetra-*n*-butylammonium hexafluorophosphate (TBAH). It was assumed that the TEAP and TBAH electrodes would give identical values.

The potential of ferrocene was measured before each compound tested. As long as the resulting redox potential was within ± 0.010 V of 0.087 V, the electrode was deemed to be working properly.

Changes in the redox potential over time are usually due to changes in the concentration of the silver ions in the reference electrode. The solution was originally 0.01 M in Ag/Ag^+ in 0.1 M TBAH CH_3CN. However, due to the instability of the ions to light, the concentration decreases over time. After the reference electrode was assembled, the redox potential of ferrocene was taken six times to ensure the 0.01 M Ag/Ag^+ reference electrode was working properly (redox potential of 0.085 ± 0.004 V). The reference electrode lasted for a month.

The electrochemical experiment showed two successive anodic and cathodic peaks, producing the radical anion and the hydroquinone dianion, respectively.[7] For each process, the reduction potential was calculated by averaging the anodic and cathodic peaks in the cyclic voltammograms. These values were corrected for ferrocene redox potential recorded before each compound scan. To convert the redox potential into SCE, 0.298 V was added.

In a reversible system the difference between the anodic and cathodic peak potentials is $\Delta E \approx 0.057/n$ V, where n is the number of electrons transferred in the reduction reaction. At low

scanning frequencies, the electrochemical equilibrium may be maintained at the electrode surface. Irreversible and quasireversible reactions have the anodic and cathodic peaks that do not coincide.[10]

This study measured the reduction potentials of a series of compounds with electron-withdrawing groups on the AQ. Structures are given in the figures (Figures 3.1 to 3.8) and reduction potentials in the tables (Table 3.1 – 3.4) at the end of this chapter. Some derivatives are not discussed explicitly in the text below; these structures are found in Figures 3.7 and 3.8.

3.1 Materials and Methods

Acetonitrile (Alfa Aesar, 99.8+ %, Ward Hill, MA), HPLC grade methanol (Caledon, 99.8 %, Ontario, Canada), tetrabutylammonium hexafluorophosphate (Aldrich, 98+ %, Milwaukee, WI), and silver nitrate (BASi, Inc., West Lafayette, IN) were used as purchased. An electrode body with Ag wire was purchased from BASi, Inc. (West Lafayette, IN).

3.1.1 Procedure for Making 0.10 M TBAH CH_3CN Solution

Clean 5.0 mL and 100.0 mL volumetric flasks were placed in an oven for 2 h at 120°C. The dried volumetric flasks, spatula, weighing boat, and TBAH were brought into the glovebox. Inside the glovebox, 3.874 g of TBAH was weighed and carefully poured into the 100.0 mL volumetric flask. A small aliquot of CH_3CN was used to wash the weighing boat of any TBAH residue. The volumetric flask was filled up half way with anhydrous CH_3CN and the flask was swirled to dissolve the TBAH. More CH_3CN was added to fill the flask up to three-fourths and the solution was swirled again to ensure that the TBAH was fully dissolved. A syringe containing anhydrous CH_3CN was used to fill the volumetric flask to the 100.0 mL line. A stirring bar was placed into the flask by using a magnet on the outside of the volumetric flask to

lower the stirring bar slowly into the TBAH solution. Then the flask was sealed with Parafilm and left to stir for 20 to 30 min inside the glovebox.

3.1.2 Procedure for Making 0.010 M Silver Nitrate ($AgNO_3$) in 0.10 M TBAH CH_3CN Solution

$AgNO_3$ was dried for 2 h. A sample of 8.494 mg $AgNO_3$ was transferred into a vial and the vial put into the glovebox. Silver nitrate was dissolved in 0.10 M TBAH CH_3CN solution using the 5.0 mL volumetric flask and the same procedure described above for making the 0.10 M TBAH CH_3CN solution.

3.1.3 Preparation and Assembly of ANE2 Electrode

The Ag wire of the ANE2 electrode was cleaned in six steps. First, a paste was made using 0.3 μm Al_2O_3 grit (Buehler, Lake Bluff, IL) and water in a weighing dish. Second, the paste was applied to the thumb and index finger of one hand. Third, the Ag wire was dragged lengthwise through the two fingers, until surface silver oxide (black in color) was fully transferred onto the fingers. Fourth, the clean Ag wire was put into a Branson 2200 Sonicator with MeOH/H_2O (1:1 v/v) for 30 min to remove most of the grit. Fifth, the wire was washed once with water. Sixth, the wire was pulled lengthwise through a Kimwipe and then blown dry with nitrogen gas. The Ag wire was transferred into the antechamber of the glovebox, where all remaining traces of absorbed water were removed.

The assembly of the ANE2 electrode body outside the glovebox was done by cutting off the used VYCOR frit. "Heat shrink" Teflon™ tubing and a Vycor frit was used to fit the seal at the bottom of the electrode body prior to putting the electrode into the glovebox. Inside the glovebox, the frit was wetted with 0.10 M TBAH CH_3CN solution, the body of the electrode was

then emptied, and 2.0 mL of a 0.010 M $AgNO_3$ in 0.10 M TBAH CH_3CN solution was added to the electrode body (see 3.1.1).

3.1.4 Ferrocene Internal Standard for CH_3CN Solutions

The ferrocene (98%, Aldrich, Milwaukee, WI) internal standard was dried for 2 h. The dried ferrocene sample (3.67 mg) was dissolved in 0.10 M TBAH CH_3CN solution, which was stirred and purged with nitrogen gas for 15 min.

After the construction of 0.01 M Ag/Ag^+ in 0.10 M CH_3CN reference electrode, ferrocene was tested using cyclic voltammetry six times.

3.1.5 Redox Potential Values for Ferrocene in 0.1 M TBAH CH_3CN

Cyclic voltammetry was used to determine the redox potential of a series of anthraquinone derivatives. In this experiment ferrocene had an average redox potential value of 0.084 ± 0.002 V.

3.2 Preparation of the Anthraquinone Samples in 0.1 M TBAH CH_3CN

Two anthraquinones were commercially available: anthraquinone-2-carboxylic acid (TCI America, 98 %, Portland, OR) and anthraquinone-2-sulfonic acid (Aldrich, 97%, Milwaukee, WI). The other anthraquinones evaluated were gifts from Reham Abou-Elkhair and Yu Cao (Georgia State University). Each sample was stirred in CH_3CN from 10 to 30 min to ensure that all the solid was fully dissolved. The surfactant solution was purged with N_2 (g) for 10 min and an inert atmosphere was kept during the experiment.

3.3 Cyclic Voltammetry of Substituted Anthraquinone Samples in 0.1 M TBAH CH_3CN

The samples were scanned from 0.00 to -2.50 V, with a scan rate of 100 mV/S, an X-sensitivity of 25 mV/cm, and a Y-sensitivity of 1.5 to 5.0 μA/cm. A three-electrode system was

used: the reference electrode was 0.010 M Ag/Ag^+ in 0.10 M TBAH CH_3CN; the working and auxiliary electrodes were platinum.

3.4 Results and Discussion

In general, the reductions of anthraquinones are reversible with the first step being AQ to $AQ^{\bullet-}$, and the second from $AQ^{\bullet-}$ to AQ^{2-}.[8] The redox potential of anthraquinone itself has been measured previously in a number of aprotic solvents. Anthraquinone in CH_3CN with a supporting electrolyte of 0.1 M tetrabutylammonium perchlorate (TBAP) gave an redox potential value of -0.911 V with an Ag/AgCl reference electrode.[11] In the same solvent with tetraethyl ammonium tetrafluoroborate (Et_4NBF), the redox potential value was -0.961 V.[4] Anthraquinone in dimethylformamide with 0.10 M TBAP gave an redox potential value of -0.831 V with a saturated calomel electrode.[12] In dimethyl sulfoxide (DMSO), anthraquinone gave an redox potential value of -0.832 V.[13] Quinones in DMSO normally have a less negative redox potential value than quinones in CH_3CN.[5] The electrolyte plays a role in the redox potential.[5,14-16] For example, anthraquinone itself has reduction potentials in acetonitrile of -0.939 and -0.911 in 0.1 M tetra-*N*-butylammonium hexafluorophosphate (this work) and 0.1 TBAP,[11] respectively. As expected, structural factors and media conditions affect the redox potential of quinones.[8]

3.4.1 Redox Potentials of Anthraquinones in 0.1 M TBAH CH_3CN.

The anthraquinone derivatives studied in this work are given in Table 3.2 to Table 3.4. The derivatives have different substituents on the 1, 2 and 3 positions of the anthraquinone moiety (Figure 3.1). In our hands, anthraquinone itself had a value of -0.939 V with an error of 0.004 V.

3.4.2 Anthraquinone Carboxamide Derivatives

We studied three monosubstituted amide anthraquinones: the *N*-methyl, *N*-propyl and *N*-*tert*-butyl carboxamide derivatives (Figure 3.2). The *N*-propyl and *N*-*tert*-butyl derivatives had redox potentials of -0.838 and -0.836 V, respectively. The *N*-methyl derivative (-0.790 V) had a less negative redox potential by approximately 45 mV. The disubstituted anthraquinone with $CONH(CH_2)_3OCH_3$ substituents (Figure 3.2) gave a less negative redox potential of -0.772 V, presumably easier to reduce due to the disubstitution.

3.4.3 Deoxyadensoine Ethanyl Anthraquinone-2,3-dimethyl ester

AQ-E-dA (Figure 3.4) gave a reduction potential of -0.935 V ± 1 mV, which was not significantly different from anthraquinone itself, -0.939 V ± 4 mV. When the two ester groups were placed on AQ-E-dA to give dA-E-AQ-2,3-CO_2CH_3 (Figure 3.4) the reduction potential decreased to -0.700 V ± 4 mV. Thus, the addition of the two ester groups gave a less negative redox potential by 235 mV. As expected, the ester groups made the anthraquinone easier to reduce.

3.4.4 Anthraquinone Carboxylic Acid Derivatives

The redox potential of $AQCO_2H$ has been measured previously,[1,17-19] including in CH_3CN [0.1 M TBAH with an Ag/AgCl reference electrode] where the value was reported as -0.707 V (vs. NHE).[1] In our hands, $AQCO_2H$ had an redox potential of -0.988 V in CH_3CN (0.1 M TBAH and Ag/Ag^+ reference electrode). Conversion of the literature value to SCE [-0.250 V correction[2] needed to convert the Ag/AgCl reference electrode data (NHE) to Ag/Ag^+ (SCE) reference electrode data] gives a value of -0.957 V. The difference of 31 mV may be due in part to differences inherent in different laboratories and in part to the difference in reference electrodes.

This redox potential of the $AQCO_2H$ (-0.988 V) was 49 mV more negative than that of AQ (-0.939 V) itself. The addition of a second carboxylic acid (AQ-2,3-CO_2H) gave an redox potential of -0.829 V. Unexpectedly, addition of one carboxylic acid made the AQ harder to reduce than the parent anthraquinone, whereas the addition of a second carboxylic acid made the compound easier to reduce than the parent anthraquinone. This is a different pattern than that observed in the ester series, where the AQ, $AQCO_2Me$, and AQ-2,3-CO_2Me had reduction potentials of -0.939, -0.785 and -0.683, respectively.

Previous work in a pyrene system has shown that the orientation of the carboxyl groups with respect to the plane of the ring has a very large effect on the redox potentials of the system.[20] Molecular models show that two substituted carbonyl groups in *ortho* positions on a benzene ring are in steric contact, leading to rotation of one or both out of the plane. A detailed computational study of benzene-1,2-dicarboxylic acid showed nine different conformers.[21] Thus, it is possible that the different conformations adopted by these various derivatives result in the apparent inconsistency in the redox potentials as a function of substituent. It is also possible that there may be an effect of aggregation in solution, even in acetonitrile.

3.4.5 Anthraquinone $COCF_3$ and its Hydrated Form

In the dA-Y-AQ series with a $COCF_3$ substituent, both the ketone itself (TBDPSOdA-Y-$AQCOCF_3$) and the hydrated form of the ketone [TBDPSOdA-Y-$AQC(OH)_2CF_3$] were available (Figure 3.3). The redox potential values of these two derivatives were not significantly different, with the former having an redox potential of -0.878 V ± 1 mV and the latter of -0.887 V ± 5 mV. It appears that one of the forms has converted to the other under the conditions of the experiment. These experiments were in dry acetonitrile. It is to be noted that in aqueous solution, it is highly likely that an anthraquinone bearing a trifluoroacetyl group would exist in

its hydrated form. In related work, the hydrated form of trifluoroacetophenone has been shown to be favored 100-fold over the keto form in aqueous solution.[22] In the trifluoroacetophenone system, reduction in water is a complex process, significantly affected by the hydration-dehydration equilibrium.[23]

3.4.6 The Effects of an Ethynyl Group on AQ Redox Potentials

Ethynyl substituents were added to three anthraquinone derivatives. In the case of the anthraquinone diester, the parent compound (AQ-2,3-CO_2CH_3, Figure 3.5) had an redox potential value of -0.683 V. Addition of an ethynyl group to the anthraquinone (Y-AQ-2,3-CO_2CH_3) gave a less negative redox potential by approximately 75 mV (-0.607 V). Thus, the compound with the ethynyl group was easier to reduce. The addition of TMS onto the ethynyl group (TMSY-AQ-2,3-CO_2CH_3) had no additional effect (-0.606 V). A third derivative was the YdA conjugate (dA-Y-AQ-2,3-CO_2CH_3); this was easier to reduce (-0.574 V) than the parent anthraquinone diester AQ-2,3-CO_2CH_3 (-0.683 V) by 109 mV.

Two other parent anthraquinone/YdA conjugate pairs were available. In the case of the parent anthraquinone itself, the YdA conjugate (AQ-Y-dA, -0.809 V) required less energy for redox to occur than AQ itself (-0.939) by 129 mV. In the case of the aldehyde-substituted AQ (Figure 3.6), the YdA conjugate (dA-Y-AQCHO, -0.639 V required less energy for redox to occur than AQCHO itself (-0.739) by 100 mV. Thus, the addition of YdA onto anthraquinone itself and a substituted anthraquinone lowered the redox potential by more than 100 mV.

3.4.7 Comparing Anthraquinones Covalently Linked (Ethynyl or Ethanyl) with dA

The addition of dA onto the ethynyl group of the AQ diester to give dA-Y-AQ-2,3-CO_2CH_3 resulted in an redox potential that was less negative by approximately 365mV (-0.574 V). In contrast, the related derivative with an ethanyl (dA-E-AQ-2,3-CO_2CH_3) rather than an

ethynyl linker had an redox potential of -0.700 V. Thus, the AQ-dA diester conjugate was approximately 126 mV easier to reduce with the ethynyl than with the ethanyl linker.

A related pair of molecules were those with anthraquinone itself conjugated to dA via the ethanyl and ethynyl linkers. The ethanyl anthraquinone conjugate (AQ-E-dA) gave an redox potential of -0.935 ± 0.001 V. The ethynyl anthraquinone (AQ-Y-dA) conjugate gave an redox potential of -0.809 ± 0.001 V. Overall, the linker plays a significant role in controlling the redox potential of the system. The ethynyl linker lowered the redox potential by 126 mV.

3.4.8 Ethynyl Linked Anthraquinone with Deoxyadenosine and Deoxyuracil

In addition to the AQ-Y-dA reported above, the reduction potential of AQ-Y-dU (Figure 3.7) was measured; the former was -0.809 V and the latter was -0.815 V. Thus, there was essentially no difference in the redox potential of theses two derivatives. These redox potentials are due to the reduction of the anthraquinone. Adenine and uracil have reduction potentials of 1.71 and 2.14 V, respectively, in acetonitrile.[24]

3.5 References

1. Ruiz, G. T.; Juliarena, M. P.; Lezna, R. O.; Wolcan, E.; Feliz, M. R.; Ferraudi, G. Shielding of electron acceptors coordinated to rhenium(I) by carboxylato groups. Intraligand and charge-transfer excited-state properties of *fac*-('anthraquinone-2-carboxylato')(2,2'-bipyridine)tricarbonylrhenium (*fac*-[Re^1(aq-2-CO_2)(2,2'-bipy)$(CO)_3$]) *Helv. Chim. Acta* **2002**, *85*, 1261-1275.

2. Pavlishchuk, V. V.; Addison, A. W. Conversion constants for redox potentials measured versus different reference electrodes in acetonitrile solutions at 25°C *Inorg. Chim. Acta* **2000**, *298*, 97-102.

3. Lehmann, M. W.; Evans, D. H. Anomalous behavior in the two-step reduction of quinones in acetonitrile *J. Electroanal. Chem.* **2001**, *500*, 12-20.

4. Frontana, C.; Vazquez-Mayagoitia, A.; Garza, J.; Vargas, R.; Gonzalez, I. Substituent effect on a family of quinones in aprotic solvents: An experimental and theoretical approach, *J. Phys. Chem. A* **2006**, 110, 9411-9419.

5. Gupta, N.; Linschitz, H. Hydrogen-bonding and protonation effects in electrochemistry of quinones in aprotic solvents *J. Am. Chem. Soc.* **1997**, *119*, 6384-6391.

6. Buschel, M.; Stadler, C.; Lambert, C.; Beck, M.; Daub, J. Heterocyclic quinones as core units for redox switches: UV-vis/NIR, FTIR spectroelectrochemistry and DFT calculations on the vibrational and electronic structure of the radical anions *J. Electroanal. Chem.* **2000**, *484*, 24-32.

7. Bauscher, M.; Mantele, W. Electrochemical and infrared-spectroscopic characterization of redox reactions of *p*-quinones *J. Phys. Chem.* **1992**, *96*, 11101-11108.

8. Aguilar-Martinez, M.; Macias-Ruvalcaba, N. A.; Bautista-Martinez, J. A.; Gomez, M.; Gonzalez, F. J.; Gonzalez, I. Review: Hydrogen bond and protonation as modifying factors of the quinone reactivity *Curr. Org. Chem.* **2004**, *8*, 1721-1738.

9. Newkome, G. R.; Narayanan, V. V.; Godinez, L. A. Electroactive, internal anthraquinonoid dendritic cores *J. Org. Chem.* **2000**, *65*, 1643-1649.

10. Bard, A. J.; Faulkner, L. R. *Electrochemical Methods: Fundamentals and Applications*; John Wiley & Sons Inc.: Hobooken, **2001**, see table on inside back cover.

11. Shamsipur, M.; Siroueinejad, A.; Hemmateenejad, B.; Abbaspour, A.; Sharghi, H.; Alizadeh, K.; Arshadi, S. Cyclic voltammetric, computational, and quantitative structure-

electrochemistry relationship studies of the reduction of several 9,10-anthraquinone derivatives *J. Electroanal. Chem.* **2007**, *600*, 345-358.

12. Ashnagar, A.; Bruce, J. M.; Dutton, P. L.; Prince, R. C. One- and two-electron reduction of hydroxy-1,4-naphthoquinones and hydroxy-9,10-anthraquinones: The role of internal hydrogen bonding and its bearing on the redox chemistry of the anthracycline antitumour quinones *Biochim. Biophys. Acta* **1984**, *801*, 351-359.

13. Jeziorek, D.; Ossowski, T.; Liwo, A.; Dyl, D.; Nowacka, M.; Woznicki, W. Theoretical and electrochemical study of the mechanism of anthraquinone-mediated one-electron reduction of oxygen: The involvement of adducts of dioxygen species to anthraquinones *J. Chem. Soc., Perkin Trans. 2* **1997**, 229-236.

14. Peover, M. E.; Davies, J. D. The influence of ion-association on the polarography of quinones in dimethylformamide *J. Electroanal. Chem.* **1963**, *6*, 46-53.

15. Dubois, D.; Moninot, G.; Kutner, W.; Jones, M. T.; Kadish, K. M. Electroreduction of buckminsterfullerene (C_{60}), in aprotic solvents, supporting electrolyte, and temperature effects *J. Phys. Chem.* **1992**, *96*, 7137-7145.

16. Abraham, M. Hydrogen-bonding. Part 9. Solute proton donor and proton acceptor scales for use in drug design *J. Chem. Soc., Perkin Trans. 2* **1989**, 1355-1375.

17. Maia, G.; Maschion, F. C.; Tanimoto, S. T.; Vaik, K.; Maeorg, U.; Tammeveski, K. Attachment of anthraquinone derivatives to glassy carbon and the electrocatalytic behavior of the modified electrodes toward oxygen reduction *J. Solid State Electrochem.* **2007**, *11*, 1411-1420.

18. Mogharrab, N.; Ghourchian, H. Anthraquinone 2-carboxylic acid as an electron shuttling mediator and attached electron relay for horseradish peroxidase *Electrochem. Commun.* **2005**, *7*, 466-471.

19. Blankespoor, R. L.; Schutt, D. L.; Tubergen, M. B.; De Jong, R. L. The influence of ion-pairing on the electroreductive cleavage of substituted 9,10-anthraquinones in DMF solution *J. Org. Chem.* **1987**, *52*, 2059-2064.

20. Kerr, C. E.; Mitchell, D.; Ying, Y. M.; Eaton, B. E.; Netzel, T. L. Synthesis and Photophysics of a 1-Pyrenylmethyl-Substituted 2'-Deoxyuridine-5-Carboxamide Nucleoside: Electron-Transfer Product Lifetimes and Energies J. Phys. Chem. B **2000**, 104, 2166-2175.

21. Fiedler, P.; Bohm, S.; Kulhanek, J.; Exner, O. Acidity of *ortho*-substituted benzoic acids: An infrared and theoretical study of the intramolecular hydrogen bonds *Org. Biomol. Chem.* **2006**, *4*, 2003-2011.

22. James Scott, W.; Zuman, P. Polarographic reduction of aldehydes and ketones part 19[a]. Hydration equilibria and their effect on reduction of α,α,α-trifluoroacetophenone *Anal. Chim. Acta* **1981**, *126*, 71-93.

23. Petr, Z. Aspects of electrochemical behavior of aldehydes and ketones in protic media *Electroanal.* **2006**, *18*, 131-140.

24. Seidel, C. A. M.; Schulz, A.; Sauer, M. H. M. Nucleobase-specific quenching of fluorescent dyes. 1. Nucleobase one-electron redox potentials and their correlation with static and dynamic quenching efficiencies *J. Phys. Chem.* **1996**, *100*, 5541-5553.

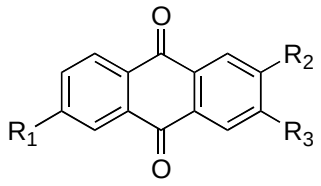

Figure 3.1: Anthraquinone indicating the numbering of the substituent position.

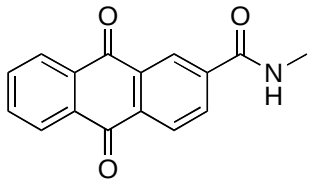

AQCONHCH$_3$

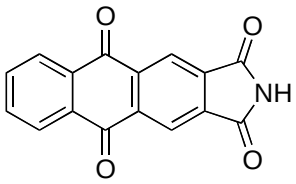

AQI

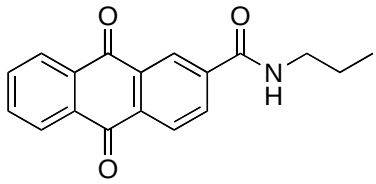

AQCONH(CH$_2$)$_2$CH$_3$

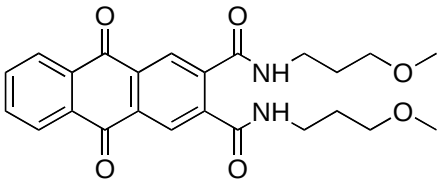

AQ-2,3-CONH(CH$_2$)$_3$OCH$_3$

Figure 3.2: Structures of selected compounds in this study. Full names are given in the List of Abbreviations.

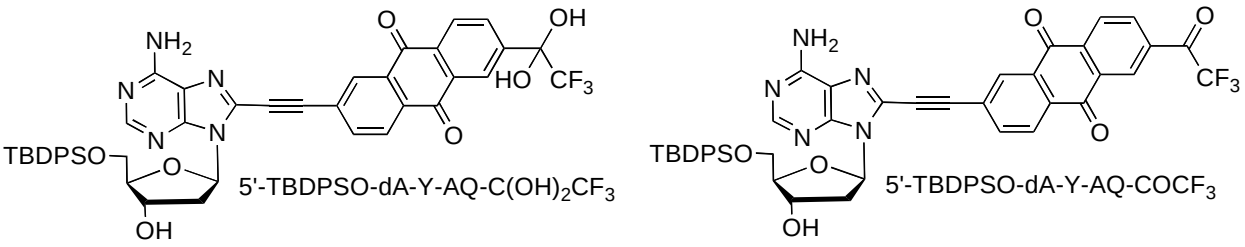

Figure 3.3: Structures of anthraquinones studied bearing $COCF_3$ substituents. Full names are given in the List of Abbreviations.

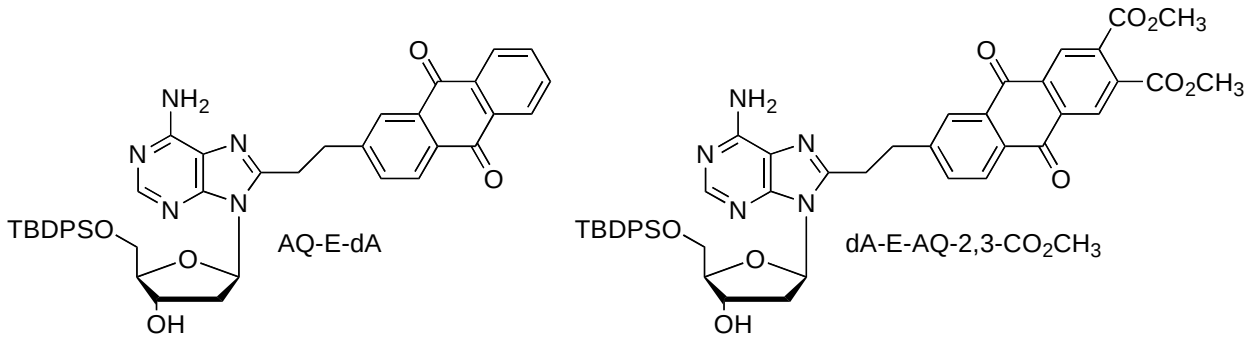

Figure 3.4: Structures of selected compounds in this study. Full names are given in the List of Abbreviations.

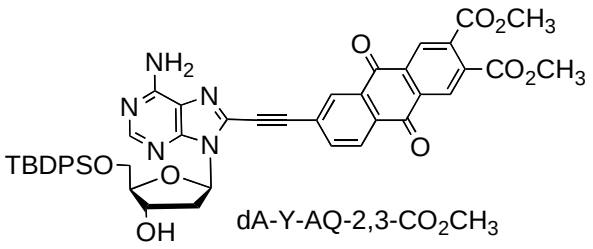

dA-Y-AQ-2,3-CO_2CH_3

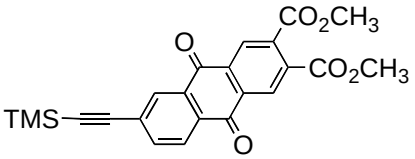

TMSY-AQ-2,3-CO_2CH_3

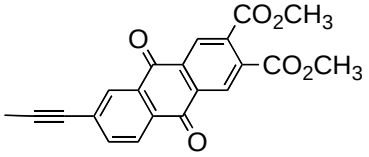

Y-AQ-2,3-CO_2CH_3

Figure 3.5: Structures of selected compounds in this study. Full names are given in the List of Abbreviations.

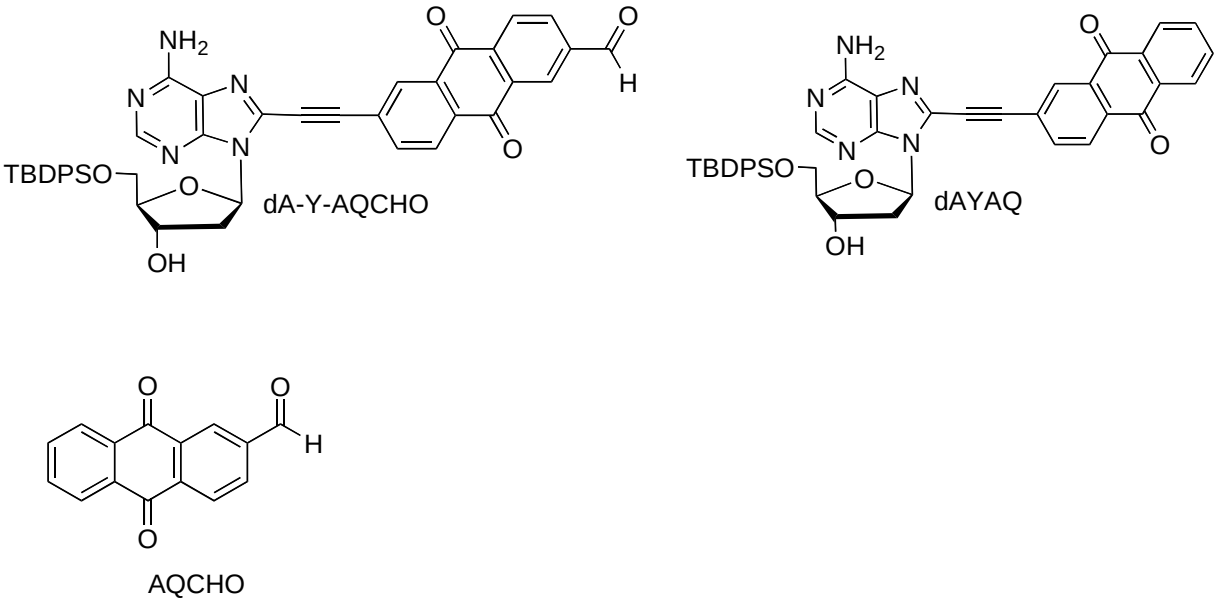

Figure 3.6: Structures of selected compounds in this study. Full names are given in the List of Abbreviations.

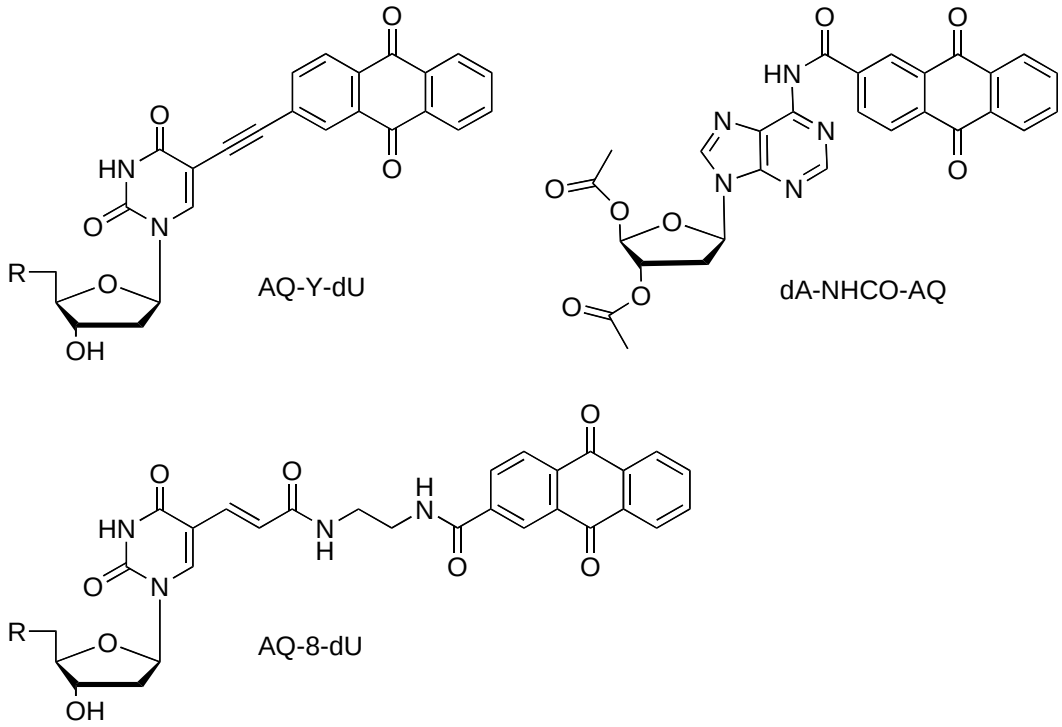

Figure 3.7: Structures of some of the compounds in this study. Full names are given in the List of Abbreviations.

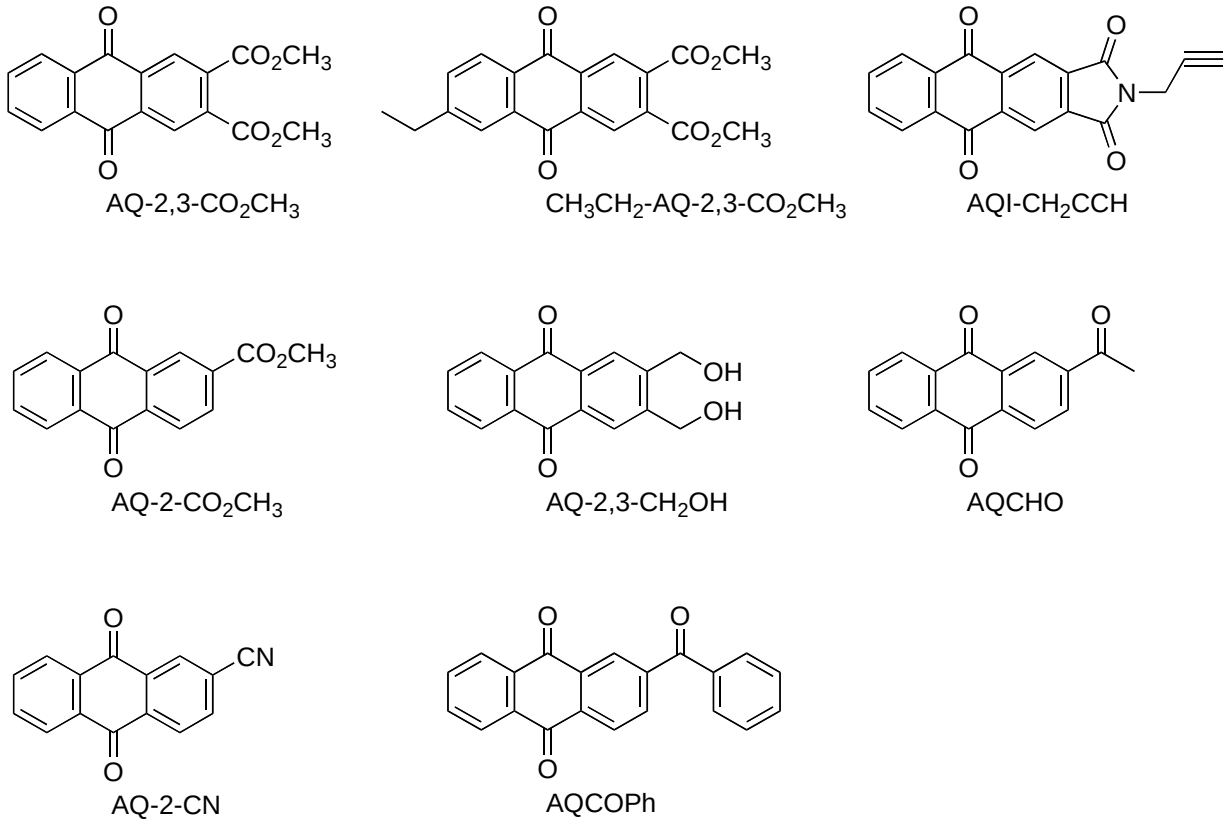

Figure 3.8: Structures of selected compounds in this study. Full names are given in the List of Abbreviations.

Table 3.1: Formula weights, sample weights and concentrations of solutions used for electrochemistry experiments.

Sample	Conc (mM)	F.W (g/mol)	Mass (mg)	0.1 M TBAH CH_3CN (mL)
Ferrocene	1.97	186.04	3.67	10.0
Anthraquinone	1.12	210.23	2.36	10.0
N-Methyl-anthraquinone-carboxamide	0.999	265.26	2.65	10.0
N-Propyl-anthraquinone-carboxamide	0.995	293.32	2.92	10.0
N-*tert*-Butyl-anthraquinone-2-carboxamide	1.04	307.43	3.19	10.0
Methoxypropyl-anthraquinone-2,3-dicarboxamide	1.10	438.47	2.42	5.0
Anthraquinone-ethanyl-deoxyadenosine	1.02	485.49	2.48	5.0
Deoxyadenosine-ethanyl-anthraquinone-2,3-dicarboxlyate	1.05	839.96	4.42	5.0
Anthraquinone-2-carboxylic acid	0.983	252.22	1.24	5.0
Anthraquinone-2,3-dicarboxylic acid	1.01	296.23	2.98	10.0
dA-ethynyl-2-trifluoroacetyl-anthraquinone	0.691	815.87	2.82	5.0
dA-ethynyl-2-trifluoroacetyl-anthraquinone, hydrate	0.597	833.88	2.49	5.0
Anthraquinone-2-carboxlyate	0.68	266.25	0.91	5.0
Anthraquinone-2,3-dicarboxlyate	0.993	324.28	3.22	10.0
Ethylyn-anthraquinone-2,3-dicarboxlyate	1.03	348.31	1.80	5.0
TMS-ethynyl-anthraquinone-2,3-dicarboxlyate	0.989	420.49	2.08	5.0
Deoxyadenosine-ethynyl-anthraquinone-2,3-dicarboxlyate	0.872	853.93	7.45	10.0
Anthraquinone-2-carbaldehyde	1.16	236.22	2.74	10.0
dA-ethynyl-anthraquinone-2-carbaldehyde	0.707	747.87	4.23	8.0
Anthraquinone-ethynyl-deoxyuracil	1.29	760.24	9.82	10.0
Anthraquinone-ethynyl-deoxyadenosine	1.00	481.46	2.41	5.0
2-Acetylanthraquione	1.03	250.25	2.58	10.0
2-Benzoylanthraquinone	1.06	312.32	3.31	10.0
Anthraquinone-CO-dA$(OAC)_2$	1.05	537.52	5.63	10.0
Anthraquinone-carboxamide-dA-dicarboxylate	1.05	537.52	5.63	10.0
Anthraquinone-$CONHCH_2NHCOCH_2CH_2$dU	1.27	876.90	3.68	5.0
2-Cyanoanthraquinone	1.15	233.22	1.34	5.0
2,3-*bis*(Hydroxymethyl)anthraquinone	1.01	268.26	1.35	5.0
Anthraquinone-2-sulfonic acid	1.12	328.28	3.67	10.0
Ethyl-anthraquinone-dicarboxlyate	1.57	352.34	2.76	5.0
N,*N*-Dipropyl-anthraquinone-2,3-dicarboxamide	1.00	380.44	1.91	5.0
1*H*-naphtho[2,3-*f*]isoindole-1,3,5,10(2*H*)-tetraone	1.03	277.23	1.42	5.0
2-(prop-2-ynyl)-1*H*-naphtho[2,3-*f*]isoindole-1,3,5,10(2*H*)-tetraone	1.11	315.28	1.79	5.0

Table 3.2: Electrochemical properties of small AQ derivatives in CH_3CN (V). [a]

Compound	E_{pa}^1	E_{pc}^1	ΔE	$E^1_{½}$	E_{pa}^2	E_{pc}^2	ΔE	$E^2_{½}$
AQ	-1.165	-1.288	0.124	-0.939	-1.791	-2.083	0.292	-1.649
AQCN	-0.971	-1.053	0.082	-0.715	-1.567	-1.779	0.212	-1.375
AQCOPh	-1.020	-1.101	0.081	-0.767	-1.591	-1.674	0.083	-1.338
AQCHO	-0.983	-1.077	0.094	-0.738	[b]	[b]	[b]	[b]
$AQCOCH_3$	-1.030	-1.126	0.096	-0.784	-1.479	-1.555	0.076	-1.219
$AQSO_3^-$	-1.135	-1.227	0.092	-0.883	[b]	[b]	[b]	[b]
$AQCONHC(CH_3)_3$	-1.080	-1.179	0.099	-0.836	-1.683	-1.857	0.174	-1.474
$AQCONHCH_3$	-1.034	-1.125	0.091	-0.790	-1.639	-1.738	0.099	-1.401
$AQCONH(CH_2)_2CH_3$	-1.094	-1.174	0.080	-0.838	-1.704	-1.851	0.088	-1.481
AQ-2,3-CO_2CH_3	-0.928	-1.023	0.095	-0.683	-1.519	-1.626	0.106	-1.278
E-AQ-2,3-CO_2CH_3	-0.966	-1.056	0.090	-0.713	-1.434	-1.636	0.202	-1.237
TMSY-AQ-2,3-CO_2CH_3	-0.846	-0.956	0.110	-0.606	-1.118	-1.242	0.124	-0.890
Y-AQ-2,3-CO_2CH_3	-0.857	-0.954	0.097	-0.607	-1.410	-1.527	0.117	-1.181

[a]Redox potentials were reported vs. SCE. [b]The second peak was irreversible.

Table 3.3: Electrochemical properties of AQ nucleosides in CH_3CN (V), reported vs. SCE.

Compound	E_{pa}^1	E_{pc}^1	ΔE	$E^1_{1/2}$
AQ-8-dU	-1.007	-1.123	0.116	-0.773
AQ-Y-dA	-1.046	-1.160	0.114	-0.809
AQ-E-dA	-1.192	-1.274	0.082	-0.935
AQ-Y-dU	-1.058	-1.166	0.108	-0.815
dA-NHCO-AQ	-0.989	-1.085	0.096	-0.742
dA-Y-AQ-2,3-CO_2CH_3	-0.835	-0.909	0.074	-0.574
dA-E-AQ-2,3-CO_2CH_3	-0.956	-1.034	0.078	-0.700

Table 3.4: Electrochemical properties of AQ substituent linker series (V).

Substituent	Parent	Parent Y	Parent E	Parent YdA	Parent EdA
2,3-CO_2CH_3	-0.683	-0.607	-0.713	-0.574	-0.700
AQ	-0.939			-0.809	-0.935
CHO	-0.739			-0.639	

Chapter 4: Synthesis, Electrochemistry and Hydrolysis of Anthraquinone Derivatives

Synthesis, Electrochemistry and Hydrolysis of Anthraquinone Derivatives

Yu Cao, Daniel J. Rabinowitz, Dabney W. Dixon,* and Thomas L. Netzel

Department of Chemistry, Georgia State University, Atlanta, Georgia, USA 30302-4098

4.0 Abstract

Anthraquinone (AQ) derivatives, including members of the anthraquinone imide (AQI) family, have been synthesized to afford good candidates for electron transfer studies in DNA. Electron withdrawing groups on the anthraquinone ring give a less negative reduction potential, as desired. As expected, the AQI derivatives have less negative reduction potentials than AQ derivatives. The AQI ring system has a half-life for hydrolysis of about 75 min in a 7:3 solution of 0.005 M of K_2CO_3 in methanol and acetonitrile.

4.1 Keywords

Electron transfer, anthraquinone bisamide, anthraquinone imide, hydrolysis, DNA

4.2 Introduction

Electron transfer resulting in oxidative damage to the DNA bases primarily occurs at guanine (G), which is the most easily oxidized of the four bases.[1] Adenine (A), with the second lowest reduction potential among all four bases has also been studied.[2-5] Recent work has shown that in DNA containing only adenine and thymine (T), only T oxidation products are seen due to the high reactivity of the $T^{\cdot+}$.[4, 5] Thus, $A^{\cdot+}$ is difficult to study because $A^{\cdot+}$ is less stable than $G^{\cdot+}$ and less reactive than $T^{\cdot+}$. Further work would be aided by electron acceptors with a relatively high driving force covalently attached to 2'-deoxyadenosine, and anthraquinone (AQ) derivatives can fulfill this objective.[6-8] The driving force can be increased by adding electron withdrawing groups or extending the conjugation of the AQ ring system. The anthraquinone

imide (AQI) is of interest in this regard because of its significantly increased driving force.[9-12] Indeed, the AQI is more favorable to formation of the radical anion than is AQ itself; in MeCN, the $E^1_{1/2}$ value[9] of the AQI is about 120 mV less negative than that of AQ itself.[10]

The goal of this study was to synthesize AQ derivatives with electron withdrawing groups and measure the electrochemical properties of these compounds. Because the long term goal of this work is to incorporate these derivatives into DNA, and this incorporation commonly uses basic conditions for cleavage from the solid supports,[13] we also studied the base-catalyzed hydrolysis of the AQI.

4.3 Results and Discussion

The AQ derivatives were synthesized as shown in Scheme 1. The AQ bisamide was prepared from dimethyl anthraquinone-2,3-dicarboxylate, while the AQI was made from either dimethyl anthraquinone-2,3-dicarboxylate or anthraquinonedicarboxylic acid anhydride. The AQ bisamide preparation requires milder conditions (lower temperature and shorter reaction time) than does AQI synthesis.

Redox potentials for the AQ derivatives are shown in Table 1. Addition of two amide groups raises the reduction potential by ≈ 170 mV, while the addition of two ester groups has a larger effect, raising the reduction potential by ≈ 260 mV with respect to AQ itself. The AQI derivatives have even less negative reduction potentials, ≈ 360 mV less negative than AQ itself. Thus, AQI derivatives have the higher driving force for electron transfer by at least 100 mV. These AQ derivatives could be elaborated into DNA base conjugates, e.g., for the amide series **4** by devising side chains which could be attached to the DNA and for the AQI **5c** by using palladium coupling chemistry to attach this molecule to a bromoadenine derivative.

Covalent attachment of these derivatives to DNA would necessitate a base deprotection step. The anthraquinone ring itself is stable to base deprotection conditions. To see if the AQI ring would also be stable, we monitored the UV-visible spectrum of AQI **5b** under basic conditions. In 3:7 MeCN and 60 mM pH = 8.0 aqueous sodium tetraborate solution, the absorbance of a sample of **5b** increased at 208 nm and decreased at 230 nm with an isosbestic point at 219 nm (Figure 1). The half-life of the hydrolysis was approximately 45 min. Base deprotection in DNA synthesis can be effected with 0.05 M K_2CO_3 in MeOH.[13] These conditions gave rapid hydrolysis of the AQI system. Even with a 10-fold lower concentration of K_2CO_3, the half-life for hydrolysis was approximately 75 min (3:7 MeCN and 0.005 M K_2CO_3 in MeOH, data not shown). Thus, the AQI ring may therefore be most useful when covalently attached to a peptide nucleic acid (PNA),[14] as this does not require the base hydrolysis step.

4.4 Experimental

4.4.1 Materials and General Methods

Chemicals were purchased from Alfa-Aesar, TCI America, and Aldrich. Thin layer chromatography (TLC) was run using 2.5 - 10.0% MeOH in CH_2Cl_2 as the eluent on Silica Gel 60 F_{254} Precoated Plates from EMD Chemicals Inc. Flash column chromatography was carried out on Sorbent Technologies silica gel (standard grade, 60 Å porosity, 230 - 400 mesh) that was packed in glass columns and pressurized with boil-off nitrogen. NMR spectra were recorded on a Brucker Avance 400 using either $CDCl_3$ or DMSO-d_6 as solvents. Mass spectra (MS) were recorded in either positive or negative ion modes on a Waters Micromass Q-TOFTM with 5 ppm accuracy. High-resolution (HR) MS were obtained with electrospray ionization (ESI). UV-visible absorbance spectra were recorded on a UV-2501PC spectrometer (Shimadzu). Melting

points were recorded via a microscope (Cambridge QUANTIMET 900) and a hot-stage (Mettler FP800); melting points are corrected.

4.4.2 Electrochemistry

Two one-electron reduction potentials of anthraquinone derivatives were measured in anhydrous acetonitrile with 0.10 M tetrabutylammonium hexafluorophosphate (TBAH) as the supporting electrolyte. The cyclic voltammograms were obtained using a CHI Instruments electrochemical workstation with a PC for data acquisition. The measurements were taken using a three-electrode system: platinum working and auxiliary electrodes and a 0.01 M Ag/Ag^+ in 0.1 M TBAH CH_3CN reference electrode. The scan rate was set to 100 mV/s. The measurements are reported in SCE. The reduction potential data of AQ itself are similar to those in acetonitrile with 0.1 M TBAP.[15] AQI derivative **5a** did not give clean reduction potential data, in line with previous studies on the phthalimide system.[16, 17]

4.3.3 Synthesis

Dimethyl anthraquinone-2,3-dicarboxylate (2)[18, 19]

Anthraquinone-2,3-dicarboxylic acid **1**[20] (3.23 g, 12.3 mmol) was esterified in refluxing anhydrous methanol (MeOH, 133 mL, 36.9 mol) containing 98% H_2SO_4 (3.2 mL) for 1 d to afford **2** (3.15 g, 89%). The ^{1}H NMR spectra matched that in the literature.[19]

***N,N'*-Dipropyl-anthraquinone-2,3-dicarboxamide (4a)**

Compound **2** (27 mg, 0.083 mmol) was dissolved in 0.5 mL THF. *n*-Propylamine (1.5 mL, 18 mmol) was added and the resulting solution was stirred at rt for 19 h. The solvent was removed under vacuum; the residue was purified via a silica gel chromatography eluted with $MeOH/CH_2Cl_2$ (0:100-2:98) to afford **4a** (31 mg, 98%) as a yellow solid: ^{1}H NMR (400 MHz, DMSO-d_6) δ 8.64 (t, J = 5.6 Hz, 2H, NH), 8.26-8.23 (m, 2H, Ar), 8.17 (s, 2H, Ar), 8.00-7.96 (m,

2H, Ar), 3.22-3.18 (m, 4H, NH$\underline{CH_2}$), 1.59-1.50 (m, 4H, $\underline{CH_2}CH_3$), 0.94 (t, J = 7.6 Hz, 6H, CH_3); ^{13}C NMR (100 MHz, DMSO-d_6) δ 182.2, 167.0, 142.1, 135.3, 133.5, 127.4, 126.3, 41.4, 22.7, 11.9; HRMS (ESI) calcd for $C_{22}H_{21}N_2O_4$ (M – H^+) 377.1501, found 377.1500. Mp 214 - 217 ^oC.

***N,N'*-Bis(3-methoxypropyl)-anthraquinone-2,3-dicarboxamide (4b)** was prepared as described above for **4a** as a pale yellow solid (79%). ^{1}H NMR (400 MHz, DMSO-d_6) δ 8.65 (t, J = 5.6 Hz, 2H, NH), 8.28-8.26 (m, 2H, Ar), 8.19 (s, 2H, Ar), 8.00-7.98 (m, 2H, Ar), 3.43 (t, J = 6.4 Hz, 4H, $\underline{CH_2}O$), 3.30-3.27 (br, 10H, $\underline{CH_3}$, NH$\underline{CH_2}$), 1.78-1.75 (m, 4H, $NHCH_2\underline{CH_2}$); ^{13}C NMR (100 MHz, DMSO-d_6) δ 182.2, 167.0, 142.0, 135.3, 133.6, 127.4, 126.3, 70.1, 58.4, 37.0, 29.5; HRMS (ESI) calcd for $C_{24}H_{27}N_2O_6$ (M + H^+) 439.1869, found 439.1886. Mp 189 - 192 ^oC.

Anthraquinone-2,3-dicarboximide (5a)[21]

Ammonium hydroxide solution (28%, 5 mL) was added to the solution of **2** (30 mg) in MeOH/THF (1:1, 4 ml) at 59 ^oC. The mixture was stirred at rt for 4 h, purified via a silica gel chromatography eluted with MeOH/CH_2Cl_2 (0:100-10:98) to afford **5a** (4 mg, 16%) as a yellow solid: ^{1}H NMR (400 MHz, DMSO-d_6) δ11.92 (s, 1H, NH), 8.45 (s, 2H, Ar), 8.29-8.27 (m, 2H, Ar), 8.02-7.99 (m, 2H, Ar); ^{13}C NMR (100 MHz, DMSO-d_6) δ 181.5, 167.9, 137.7, 136.6, 135.1, 132.9, 127.1, 120.8.

***n*-Propargyl-anthraquinone-2,3-dicarboximide (5c)**

Anthraquinonedicarboxylic acid anhydride (**3**)[22] (30 mg, 0.11 mmol), anhydrous DMF (3.0 ml), and propargylamine (7.3 μL, 0.11 mmol) were sequentially added to a flask under nitrogen. The resulting mixture was stirred at 80 ^oC under nitrogen for 3.5 d, dried under vacuum, and separated by a silica gel chromatography eluted with MeOH/CH_2Cl_2 (0:100-2:98) to afford **5c** (16 mg, 47%) as a yellow solid: ^{1}H NMR (400 MHz, $CDCl_3$) δ 8.82 (s, 2H, Ar), 8.38-8.34 (m, 2H, Ar), 7.90-7.85 (m, 2H, Ar), 4.52 (d, J = 2.4 Hz, 2H, CH_2), 2.25 (t, J = 2.4 Hz,

1H, C<u>CH</u>); ^{13}C NMR (100 MHz, $CDCl_3$) δ 181.4, 165.2, 138.2, 135.7, 135.0, 133.1, 127.8, 123.0, 72.1, 27.1; HRMS (ESI) calcd for $C_{19}H_9NO_4$ (M^-) 315.0532, found 315.0540. Mp 271 - 274 ^oC.

***N*-(3-methoxypropyl)-anthraquinone-2,3-dicarboximide (5b)** was prepared as described above for **5c** as a yellow solid (21%). ^{1}H NMR (400 MHz, $CDCl_3$) δ 8.77 (s, 2H, Ar), 8.38-8.33 (m, 2H, Ar), 7.89-7.84 (m, 2H, Ar), 3.86 (t, J = 6.8 Hz, 2H, $\underline{CH_2}O$), 3.44 (t, J = 6.0, 2H, $N\underline{CH_2}$), 3.26 (s, 3H, CH_3), 2.00-1.94 (m, 2H, $NHCH_2\underline{CH_2}$); ^{13}C NMR (100 MHz, $CDCl_3$) δ 181.6, 166.6, 138.0, 136.0, 134.9, 133.1, 127.7, 122.5, 70.2, 58.7, 36.4, 28.4; HRMS (ESI) calcd for $C_{20}H_{15}NO_5$ (M^-) 349.0950, found 349.0951. Mp 236 - 239 ^oC.

4.5 Acknowledgements

The authors are grateful to Drs. Reham Abou-Elkhair, Gangli Wang and Siming Wang for fruitful discussions and to Dr. Eric Mintz for technical assistance.

4.6 References

1. Steenken, S.; Jovanovic, S. V. How easily oxidizable is DNA? One-electron reduction potentials of adenosine and guanosine radicals in aqueous solution. *J. Am. Chem. Soc.* **1997**, *119*, 617-618.

2. Giese, B.; Amaudrut, J.; Kohler, A. K.; Spormann, M.; Wessely, S. Direct observation of hole transfer through DNA by hopping between adenine bases and by tunnelling. *Nature* **2001**, *412*, 318-320.

3. Kawai, K.; Osakada, Y.; Fujitsuka, M.; Majima, T. Hole transfer in DNA and photosensitized DNA damage: Importance of adenine oxidation. *J. Phys. Chem. B* **2007**, *111*, 2322-2326.

4. Joy, A.; Ghosh, A. K.; Schuster, G. B. One-electron oxidation of DNA oligomers that lack guanine: Reaction and strand cleavage at remote thymines by long-distance radical cation hopping. *J. Am. Chem. Soc.* **2006**, *128*, 5346-5347.

5. Ghosh, A.; Joy, A.; Schuster, G. B.; Douki, T.; Cadet, J. Selective one-electron oxidation of duplex DNA oligomers: Reaction at thymines. *Org. Biomol. Chem.* **2008**, *6*, 916-928.

6. Tierney, M. T.; Grinstaff, M. W. Synthesis and stability of oligodeoxynucleotides containing C8-labeled 2'-deoxyadenosine: Novel redox nucleobase probes for DNA-mediated charge-transfer studies. *Org. Lett.* **2000**, *2*, 3413-3416.

7. Abou-Elkhair, R. A. I.; Netzel, T. L. Synthesis of two 8-[(anthraquinone-2-yl)-linked]-2'-deoxyadenosine 3'-benzyl hydrogen phosphates for studies of photoinduced hole transport in DNA. *Nucleosides Nucleotides & Nucleic Acids* **2005**, *24*, 85-110.

8. Hussein, Y. H. A.; Anderson, N.; Lian, T. T.; Abdou, I. M.; Strekowski, L.; Timoshchuk, V. A.; Vaghefi, M. M.; Netzel, T. L. Solvent and linker influences on $AQ^{\cdot-}/dA^{\cdot+}$ charge-transfer state energetics and dynamics in anthraquinonyl-linker-deoxyadenosine conjugates. *J. Phys. Chem. A* **2006**, *110*, 4320-4328.

9. Todd, E. K.; Wang, S.; Wan, X.; Wang, Z. Y. Chiral imides as potential chiroptical switches: Synthesis and optical properties. *Tetrahedron Lett.* **2005**, *46*, 587-590.

10. Shamsipur, M.; Siroueinejad, A.; Hemmateenejad, B.; Abbaspour, A.; Sharghi, H.; Alizadeh, K.; Arshadi, S. Cyclic voltammetric, computational, and quantitative structure-electrochemistry relationship studies of the reduction of several 9,10-anthraquinone derivatives. *J. Electroanal. Chem.* **2007**, *600*, 345-358.

11. Qiao, W.; Zheng, J.; Wang, Y.; Zheng, Y.; Song, N.; Wan, X.; Wang, Z. Y. Efficient synthesis and properties of novel near-infrared electrochromic anthraquinone imides. *Org. Lett.* **2008**, *10*, 641-644.

12. Breslin, D. T.; Coury, J. E.; Anderson, J. R.; McFailIsom, L.; Kan, Y. Z.; Williams, L. D.; Bottomley, L. A.; Schuster, G. B. Anthraquinone photonuclease structure determines its mode of binding to DNA and the cleavage chemistry observed. *J. Am. Chem. Soc.* **1997**, *119*, 5043-5044.

13. Venkatesan, N.; Kim, S. J.; Kim, B. H. Novel phosphoramidite building blocks in synthesis and applications toward modified oligonucleotides. *Curr. Med. Chem.* **2003**, *10*, 1973-1991.

14. Armitage, B.; Koch, T.; Frydenlund, H.; Orum, H.; Batz, H. G.; Schuster, G. B. Peptide nucleic acid-anthraquinone conjugates: Strand invasion and photoinduced cleavage of duplex DNA. *Nucleic Acids Res.* **1997**, *25*, 4674-4678.

15. Shamsipur, M.; Siroueinejad, A.; Hemmateenejad, B.; Abbaspour, A.; Sharghi, H.; Alizadeh, K.; Arshadi, S. Cyclic voltammetric, computational, and quantitative structure–electrochemistry relationship studies of the reduction of several 9,10-anthraquinone derivatives. *J. Electroanal. Chem.* **2007**, *600*, 345-358.

16. Leedy, D. W.; Much, D. L. Cathodic reduction of phthalimide systems in nonaqueous solutions. *J. Am. Chem. Soc.* **1971**, *93*, 4264-4270.

17. Orzeszkoa, A.; Maurin, J. K.; Niedźwiecka-Kornaś, A.; Kazimierczuk, Z. The novel product of cathodic reduction of phthalimide anion. *Tetrahedron* **1998**, *54*, 7517-7524.

18. Tarnchompoo, B.; Thebtaranonth, C.; Thebtaranonth, Y. 2,3-Dicarbomethoxy-1,3-butadiene and its reactions. *Tetrahedron Lett.* **1987**, *28*, 6671-6674.

19. Mehta, G.; Viswanath, M. B.; Jemmis, E. D.; Sastry, G. N. An approach to functionalized cubanes. Regioselectivities and frontier molecular orbital analysis in the addition of dimethyl cyclobutadiene-1,2-dicarboxylate to quinones. *J. Chem. Soc., Perkin Trans. 2* **1994**, 433-436.

20. Lohier, J. F.; Wright, K.; Peggion, C.; Formaggio, F.; Toniolo, C.; Wakselman, M.; Mazaleyrat, J. P. Synthesis of protected derivatives and short peptides of antAib, a novel C^{α}-tetrasubstituted α-amino acid of the Ac_5c type possessing a fused anthracene fluorophore. *Tetrahedron* **2006**, *62*, 6203-6213.

21. Willgerodt, C.; Maffezzoli, F. Anthraquinone-*O*-dicarboxylic anhydride. *J. Prakt. Chem.* **1911**, *82*, 205-231.

22. Fairbourne, A. The *ortho*-dimethylanthraquinones and their derivatives. *J. Chem. Soc.* **1921**, *119*, 1573-1583.

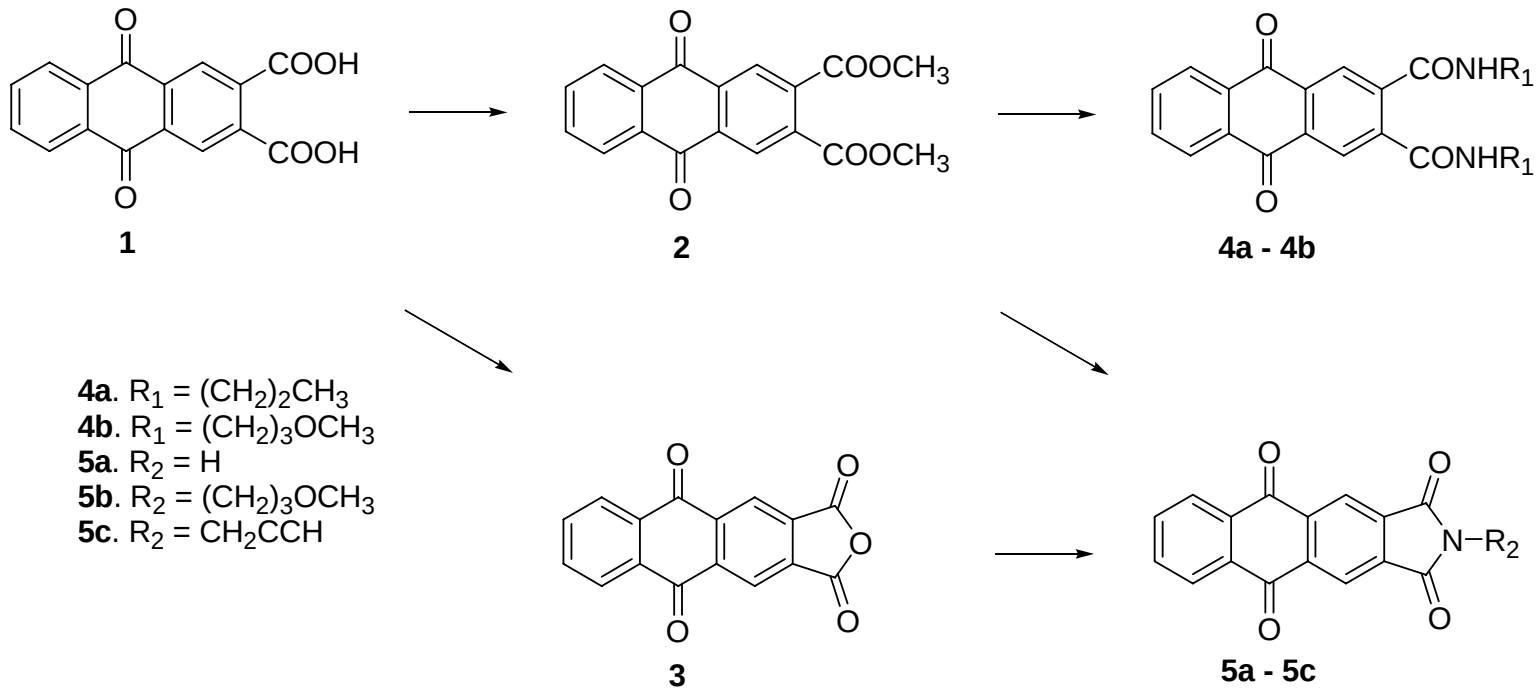

Figure 4.1 Structures of molecules investigated.

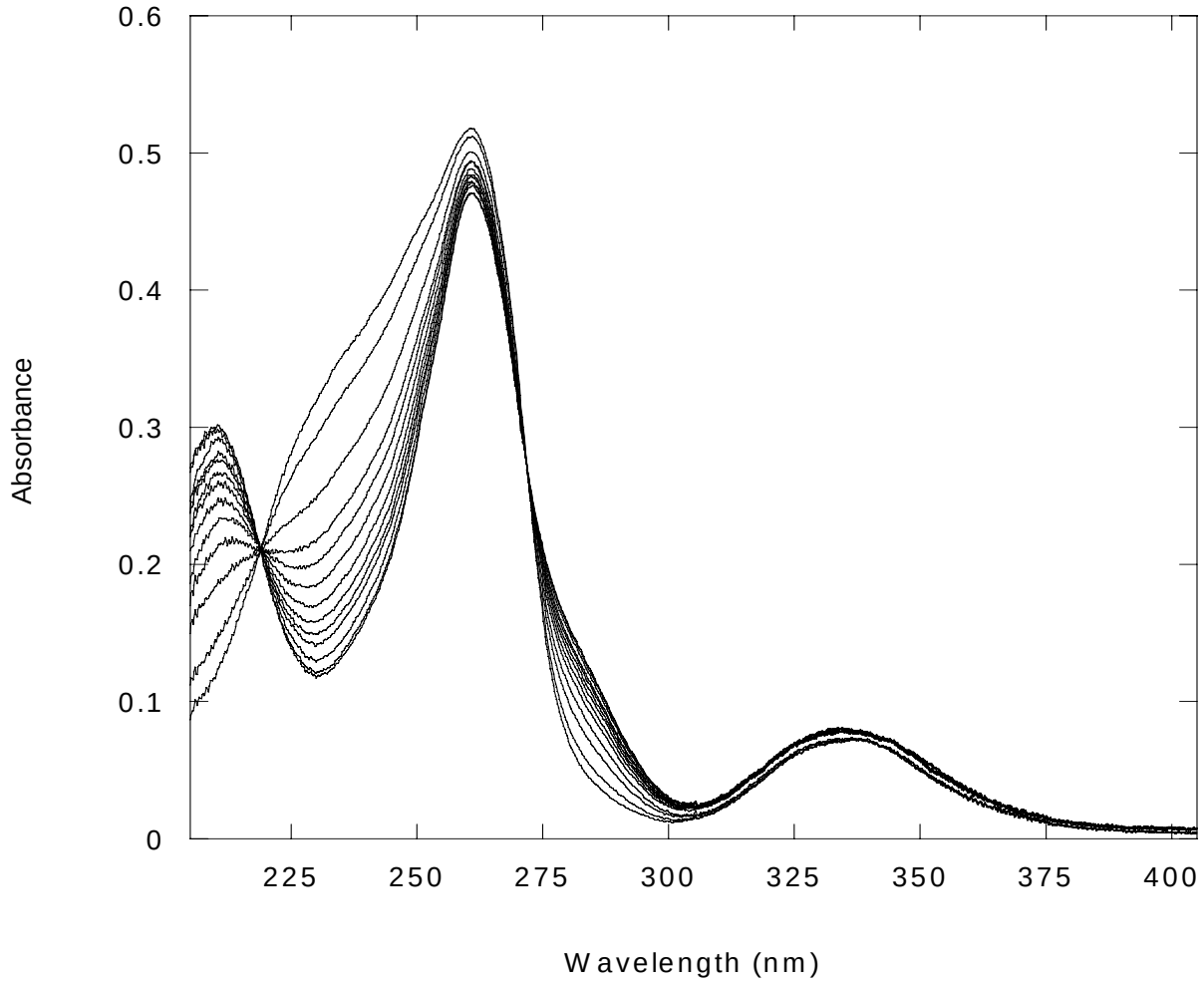

Figure 4.2 UV-visible absorbance spectra of AQI **5b** as a function of time at room temperature (3:7 MeCN and 60 mM pH = 8.0 borate buffer). Scans were taken every 15 min for the first 2 h and every 1 h for the last 3 h. The absorbance increased at 208 nm and 285 nm, and decreased at 230 nm.

Table 4.1 Reduction potentials of AQ derivatives in acetonitrile (1 mM AQ with 0.1 M TBAH).

Compound	$E^1_{½}$	$E^2_{½}$
AQ	-0.939	-1.658
1	-0.829	-1.428
2	-0.683	-1.278
4a	-0.772	-1.393
4b	-0.767	-1.361
5b	-0.595	-1.134
5c	-0.556	-1.102

Table 4.2: Electrochemical properties of AQ diamide and AQ imide derivatives in CH_3CN (V).

Compound	$E_p^a{}_1$	$E_p^c{}_1$	ΔE	$E^1{}_{½}$	$E_p^a{}_2$	$E_p^c{}_2$	ΔE	$E^2{}_{½}$
4a	-1.023	-1.111	0.088	-0.772	-1.615	-1.759	0.144	-1.393
4b	-1.019	-1.102	0.083	-0.767	-1.578	-1.735	0.143	-1.361
5b	-0.848	-0.931	0.083	-0.595	-1.377	-1.485	0.108	-1.134
5c	-0.811	-0.897	0.086	-0.556	-1.354	-1.447	0.087	-1.102

This paper was submitted to the Journal of Synthetic Communications on September 18, 2008. The paper was written by Yu Cao. The melting points, NMR and synthesis were done by Yu Cao. The electrochemical measurements were done by Daniel Rabinowitz.

Chapter 5: Theory and Experiment

5.0 Introduction

It was of interest to gain insight into some of the unexpected redox potential values in this work by comparing experiment with theoretical calculations. Previous studies have focused on anthraquinones with electron donating groups. They have calculated redox potentials[1-4] and HOMO-LUMO energies[2,5,6] using density function theory (DFT) calculations.[1,2,4,5,7,8]

Our group has focused on anthraquinones substituted with electron withdrawing groups. We have performed DFT calculations on eleven anthraquinone derivatives [AQCO_2H, AQ-2,3-CO_2H, AQCO_2CH_3, AQCHO, AQCONHCH_3, AQ-2,3-CO_2CH_3, AQCOCH_3, AQCOPh, AQ, AQCN, and AQCONHC$(CH_3)_3$] to give electron affinity values in gas phase. The electron affinity values have been compared to the redox potential values in acetonitrile.

5.1 Methods

5.1.1 Gaussian 03

The study was carried out using GAUSSIAN and GAUSSIAN 03W. GAUSSIAN 03W was used to build the anthraquinone-substituted compounds. The anthraquinone derivates were all constructed in the same manner (Figure 4.1), with the carbonyl group of the substituent group parallel to the internal keto group of the anthraquinone. Molecules with two carbonyl-based substituents were constructed in the same way. The gas phase optimization and frequency calculation was carried out at the B3LYP/6-31(G)d level of theory. For each compound, calculations were performed for both the neutral form and the form with one additional electron.

5.1.2 Calculation of Electron Affinity

The gas phase calculations were executed at 0 K. The internal energies were calculated for both the neutral form and the form with one additional electron, and the values were given by

Gaussian 03 in Hartree units. Hartees were converted into eV by multiplying the Hartree value by 27.2113838668 eV.

The electron affinity is the energy required to add an electron to the anthraquinone to create the anionic species. The electron affinity (EA) is calculated as:

$$EA = [IE(AQ) + ZPE^*(AQ)] - [IE(AQ^-) + ZPE^*(AQ^-)]$$

where IE is the internal energy of the species, and the ZPE* are the zero point energies at 0 K multiplied by the standard Gaussian 03 correction of 0.9804.[9] This study did not use the thermal energy correction which would be necessary to report calculations at 298 K.

The zero point energy (ZPE) is the residual motion of the energy of a particle in quantum mechanics. The zero point energy is the lowest state accessible to the system that has a nonzero energy. The zero point energies must be included due to the Heisenberg uncertainty principle. Classical mechanics states that when the particle is at the bottom of the well, the position is known and the momentum of a particle is zero. In quantum mechanics, neither the position nor the momentum of the particle is precisely measured. The Heisenberg uncertainty principle states that $\Delta p \Delta x \geq h/4\pi$ where Δp is the change in momentum and Δx is the change in position.[10]

5.2 Results and Discussion

The electron affinity and redox potential values for 11 compounds are reported in Table 5.1. The anthraquinone substituents that gave the highest electron affinities also generally gave the lowest redox potential values (Figure 5.2). Compounds with substituents that do not have the capability to hydrogen bond gave an excellent correlation between theory and experiment with a correlation coefficient squared (R^2) of 0.968 (Table 5.2).

For the ester and amide substituents, which can hydrogen bond, theory did not correlate well with experiment. The AQ bearing carboxylic acid substituents appeared above the line,

whereas those bearing amide substituents appeared below the correlation line (Figure 5.2). Correlation coefficients for linear fittings excluding the carboxylic acids only and excluding both the amides and carboxylic acids are given in Table 5.2.

Part of the explanation for the observation that the carboxylic acids and amides lie off the line is that these compounds presumably have some intermolecular hydrogen bonding in solution that is not reproduced in the gas phase calculations In addition, derivatives with carbonyl substituents have more than one conformation (e.g., with the carbonyl substituent parallel to the internal ketone or rotated by 120°). The situation becomes more complex when there are two carbonyl-based substituents *ortho* to one another. Each ketone substituent has two orientations and the ketone moieties are close enough in space that they cannot both lie in the plane, but one of both must be rotated out of the plane of the anthraquinone. A recent study has found that there are nine different energy minima for 1,2-benzene dicarboxylic acid.[8] In this study, we looked at only a single energy minimum for each compound.

5.3 References

1. Namazian, M.; Almodarresieh, H. A. Computational electrochemistry: Aqueous two-electron reduction potentials for substituted quinones *J. Mol. Struct. Theochem.* **2004**, *686*, 97-102.

2. Namazian, M.; Almodarresieh, H. A.; Noorbala, M. R.; Zare, H. R. DFT calculation of redox potentials for substituted quinones in aqueous solution *Chem. Phys. Lett.* **2004**, *396*, 424-428.

3. Shamsipur, M.; Siroueinejad, A.; Hemmateenejad, B.; Abbaspour, A.; Sharghi, H.; Alizadeh, K.; Arshadi, S. Cyclic voltammetric, computational, and quantitative structure-

electrochemistry relationship studies of the reduction of several 9,10-anthraquinone derivatives *J. Electroanal. Chem.* **2007**, *600*, 345-358.

4. Namazian, M. Accurate calculation of absolute one-electron redox potentials of some *para*-quinone derivatives in acetonitrile *J. Phys. Chem. A* **2007**, *111*, 7227-7232.

5. Namazian, M. Density functional theory response to the calculation of redox potentials of quinones in non-aqueous solution of acetonitrile *J. Mol. Struct. Theochem.* **2003**, *664*, 273-278.

6. Heffner, J. E.; Raber, J. C.; Moe, O. A.; Wigal, C. T. Using cyclic voltammetry and molecular modeling to determine substituent effects in the one-electron reduction of benzoquinones *J. Chem. Educ.* **1998**, *75*, 365-367.

7. Cape, J. L.; Bowman, M. K.; Kramer, D. M. Computation of the redox and protonation properties of quinones: Towards the prediction of redox cycling natural products *Phytochem.* **2006**, *67*, 1781-1788.

8. Fiedler, P.; Bohm, S.; Kulhanek, J.; Exner, O. Acidity of *ortho*-substituted benzoic acids: An infrared and theoretical study of the intramolecular hydrogen bonds *Org. Biomol. Chem.* **2006**, *4*, 2003-2011.

9. Foresman, J. B.; Frisch, A. *Exploring Chemistry with Electronic Structure Methods*; Gaussian, Inc: Pittsburgh, **1996**, 62-68

10. Engel, T. *Quantum Chemistry & Spectroscopy*; Benjamin Cummings: San Francisco, **2006**, 86-92.

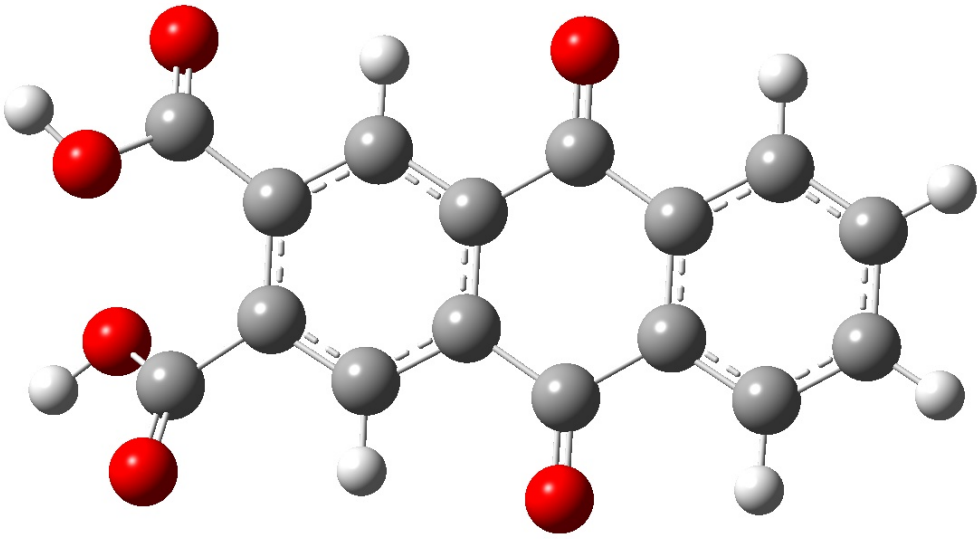

Figure 5.1: Anthraquinone-2,3-dimethyl ester structural drawing in Gaussian 03W.

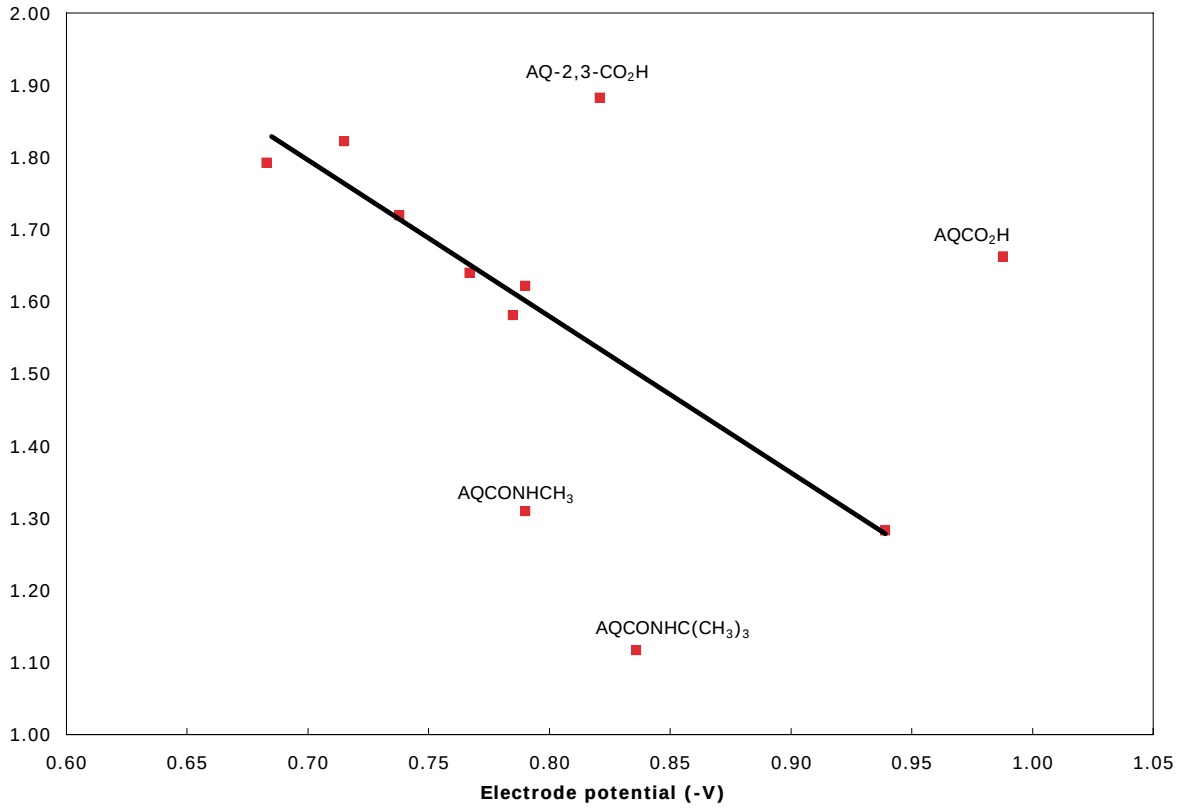

Figure 5.2: Electron affinity (eV) versus redox potential values (-V).

Table 5.1: Redox potentials, and electron affinity values.

Sample	$E_{1/2}$ exp (V)	EA (eV)
$AQCO_2CH_3$	-0.785	1.58081
AQCHO	-0.749	1.71933
$AQCONHCH_3$	-0.793	1.30914
AQ-2,3-CO_2CH_3	-0.680	1.82240
AQCN	-0.714	1.82229
AQ	-0.939	1.28270
$AQCONHC(CH_3)_3$	-0.828	1.12192
$AQCOCH_3$	-0.785	1.62175
AQCOPh	-0.769	1.63954
$AQCO_2H$	-0.988	1.66238
AQ-2,3-CO_2H	-0.821	1.88223

Table 5.2: Correlation coefficients for the electron affinity (eV) versus redox potential values (-V) as a function of the substituents excluded.

Excluded substituents	(R^2) Correlation coefficient squared
Amides and carboxylic acids	0.968
Carboxylic acids only	0.677
None	0.176

Chapter 6: Conclusions

Two pairs of AQ-dA with ethanyl and ethynyl linkers were studied, those with no substituent on the AQ, and a diester substituent. Overall, there was a distinguishable pattern of the effect of the ethynyl linker on the reduction potential, with the ethanyl derivative being harder to reduce. For example AQYdA gave a less negative redox potential than AQEdA in water and acetonitrile solutions, by 30 and 117 mV, respectively. For dA-Y-AQ-2,3-CO_2CH_3 it gave a less negative redox potential than dA-E-AQ-2,3-CO_2CH_3 in acetonitrile by 126 mV.

In acetonitrile, substitution of the AQ with one the carboxylic acid resulted in a compound that was more difficult to reduce by 49 mV. The AQ disubstituted carboxylic acid was less difficult to reduce by 118 mV. The AQ monoester was less difficult to reduce by 154 mV, while the AQ diester was less difficult to reduce by 259 mV. Thus, three of these derivatives showed the expected effect, with substitution lowering the reduction potential; the AQCO_2H was an exception. It may be that the orientation of the carbonyl group of the substituents on anthraquinone has a substantial influence on the reduction potential.

Overall, the biggest effect seen in the AQ series itself was 331 mV for an AQ diester conjugate with an ethynyl linker. An even bigger effect of 383 mV was observed for the anthraquinone imide, presumably arising from the extended conjugation of this molecule.

Electron affinity calculations were performed. Excluding the amide and carboxylic acid substituents, there was a good correlation between the electron affinity and the reduction potential. These two substituents are the only ones that can undergo hydrogen bonding in solution [assuming that the *tert*-butyl group in CONHC$(CH_3)_3$ blocks hydrogen bonding]; it is possible that hydrogen bonding has a significant effect on the reduction potential.

In summary, we have shown that it is possible to increase the driving force for electron transfer to the anthraquinone substantially by adding electron withdrawing substituents to the ring. We have also shown that experimental evaluation of the reduction potentials is vital, as the cumulative effects of hydrogen bonding of the substituted AQ, rotational isomers of carbonyl substituents, the nature of the AQ-dA linker, and solvent make it very difficult to predict the reduction potential in advance. The new derivatives described herein, with significant driving forces for electron transfer, should allow new discoveries in the field of DNA oxidation.